Numerical Simulation for Steady Incompressible/Compressible Flows of Viscous and Nanofluids

by

Muhammad Irfan

A dissertation submitted in partial fulfillment of the requirements

for the degree of Master of Philosophy in Mathematics

Supervised by

Muhammad Asif Farooq

School of Natural Sciences

National University of Sciences and Technology

Islamabad, Pakistan

January 2014

Dedicated

to

My All Family

Abstract

This dissertation has two parts. In the first part we discuss nanofluid over a stretching sheet while taking thermal radiation effect into account. In the second part, we consider the boundary layer flow of compressible fluid on a moving flat plate. The governing partial differential equations (PDEs) in both parts are reduced into the system of non-linear ordinary differential equations (ODEs) while considering appropriate similarity transformations. The numerical solutions of the resulting non-linear ODEs are obtained by shooting method with the fifth order Runge-Kutta time integration technique and the results are compared with the built-in solver bvp4c of MATLAB. Graphs are drawn for the influence of various parameters on the flow field. The present analysis of the first part shows the effects of velocity ratio and magnetic parameter on the flow of the field and effect of Prandtl and Lewis number on the temperature and concentration profile, respectively. In the second part of the thesis, the non-linear ODEs are solved by applying the shooting method and the bvp4c. We find a good agreement between the present results and the results in the literature.

Preface

Nanofluids has become an active field of research due to its applications in technological and industrial processes. Applications of nanofluids include transportation, electronic cooling, solar panels to name a few. Research on nanofluid has potential to improve the heat transfer and solar collection process by addition of nanoparticles in the base fluid. The size of these nanoparticles in diameter is less than 100 nm. The other field of research is the topic of compressible fluids. Application of compressible fluids include high speed flows around aeroplane. The arrangement of the dissertation is as follows:

Chapter 1 is introductory in nature. It presents some basic definitions and governing laws. Some details about the shooting method and bvp4c method is also part of this chapter.

Chapter 2 is the review work of Meraj et al [7]. It is concerned with the thermal radiation effect in the magnetohydrodynamic (MHD) stagnation-point flow of nanofluids towards a stretching sheet. First we convert partial differential equation (PDEs) into system of non-linear ODEs and then solve these system of non-linear ODEs by using shooting method and bvp4c. The numerical analysis of the obtained results is presented at the end of this chapter.

Chapter 3 is an extension of Meraj et al [7]. It is concerned with the thermal radiation effect in the magnetohydrodynamic (MHD) stagnation-point flow of nanofluids towards a stretching sheet with convective boundary condition. An approximate as well as the numerical solution of the problem is obtained with the help of shooting method and bvp4c. A discussion about the obtained

results is presented at the end of this chapter.

Chapter 4 is the review work of Bachok et al [9]. This chapter is the analysis of the boundary layer flow with variable fluid properties on a moving flat plate in a parallel free stream. The nonlinear ODEs are solved by applying shooting method and bvp4c. The results are discussed.

Chapter 5 contains the conclusion of the thesis and future work.

Acknowledgment

First and foremost I wish to express my deepest gratitude to my supervisor, Muhammad Asif Farooq for his guidance, advice and encouragement throughout the preparation of this dissertation. Furthermore, I would like to thank all those who have assisted me directly or indirectly towards the completion of this dissertation. I would also like to thank the GEC members Dr. Moniba Shams (SNS), Dr. Meraj Mustafa (SNS) and Dr. Adnan Maqsood (RCMS).

Finally, I would like to express my extreme gratitude and thanks to all my family members especially my parents. Without their moral support and care it would have been impossible for me to finish this work.

Contents

Chapter 1

Introduction

This chapter includes basic definitions in fluid dynamics. Some of these definitions have been used in the thesis.

1.0.1 Nanofluid

The nanofluids are a relatively new class of fluids which consist of base fluid with nanometer sized particle (1-100 nm) suspended within them. The nanoparticles used in nanofluids are typically made of metals, oxides, carbides, or carbon nanotubes. Common base fluids include water, ethylene glycol and oil. Nanofluids are useful in many applications in heat transfer including microelectronics, fuel cells, biomedicine, engine cooling, domestic refrigerator, chiller, heat exchanger, nuclear reactor coolant.

1.0.2 Stress

Stress is defined as force per unit area. Mathematically, it can be written as

$$\mathrm{P} = \frac{F}{A}, \tag{1.0.1}$$

where F is the applied force and A is the area where the force is applied.

1.0.3 Shear Stress (Tangential Stress)

The components of stress, when the fluid is in motion, tangential to the area considered.

1.0.4 Normal Stress

The components of stress, when the fluid is in motion or static, perpendicular to the area considered.

1.0.5 Stress Tensor Matrix

Stresses in a medium results from forces acting on some portion of the medium. The force δF acting on δA may be resolved into two components, one tangent to and the other normal to the area. A shear stress τ and a normal stress σ are defined as

$$\tau = \lim_{\delta A_n \to 0} \frac{\delta F_t}{\delta A_n}, \tag{1.0.2}$$

$$\sigma = \lim_{\delta A_n \to 0} \frac{\delta F_n}{\delta A_n}. \tag{1.0.3}$$

There are nine components of the stress matrix which are defined at a point in a following way

$$\tau = \begin{pmatrix} \sigma_{xx} & \sigma_{xy} & \sigma_{x_z} \\ \sigma_{yx} & \sigma_{yy} & \sigma_{yz} \\ \sigma_{zx} & \sigma_{zy} & \sigma_{zz} \end{pmatrix}.$$

1.0.6 Dynamic Viscosity

The fraction of the shear stress to the rate of strain is known as dynamic viscosity. It is denoted by μ. Mathematically

$$\mu = \frac{\text{shear stress}}{\text{strain rate}}. \tag{1.0.4}$$

The unit of dynamic viscosity is $\frac{kg}{ms}$.

1.0.7 Deformation Rate

Deformation rate or shear strain rate of an element is defined as the rate of decrease of the angle formed by two mutually perpendicular lines on the element. Mathematically

$$e_{ij} = \frac{1}{2}(\frac{\partial u_i}{\partial x_j} + \frac{\partial u_j}{\partial x_i}). \tag{1.0.5}$$

1.0.8 Newton's Law of Viscosity

Newton's law of viscosity states that shear stress is directly and linearly proportional to the deformation rate. Mathematically

$$\tau = \mu \frac{du}{dy}, \tag{1.0.6}$$

where μ is known as proportionality constant, dynamic constant or coefficient of viscosity.

1.0.9 Kinematic Viscosity

The fraction of dynamic viscosity to the density is called kinematic viscosity. It is defined by

$$\nu = \frac{\mu}{\rho}. \tag{1.0.7}$$

The unit of kinematic viscosity is m^2/t.

1.1 Types of Flows

There are few important types of flows given below.

1.1.1 Steady Flow

If the flow velocity at any point does not change with time then the flow is called steady.

1.1.2 Unsteady Flow

If the flow velocity change with time then the flow is called unsteady.

1.1.3 Laminar Flow

In laminar flow, velocity at a given point remains a smooth function of time.

1.1.4 Viscous Flow

Viscous flow are those flow in which fluid friction has significant effects.

1.1.5 Inviscid Flow

Inviscid flows are those flows in which there is no fluid friction or in other words μ=0. For instance, gases are an example of an inviscid fluids.

1.1.6 Incompressible Flow

If the density ρ does not change with space and time then the flow is incompressible. Mathematically

$$\frac{d\rho}{dt} = 0. \tag{1.1.1}$$

1.1.7 Compressible Flow

If the density ρ changes when the pressure is applied on a fluid then the flow is said to be compressible.

1.2 Type of Forces

There are four important types of forces given below.

1.2.1 Surface Forces

Surfaces forces are exerted on an area element by the surroundings through direct contacts. For example pressure force, viscous force etc.

1.2.2 Body Forces

The forces that arises from action at a distance without physical contacts are called body forces. Gravity, electric or magnetic forces are examples of body forces.

1.2.3 Inertial Forces

Inertial forces are defined as body's resistance to the forces acting on it to displace.

1.3 Types of Fluids

There are three kinds of fluids.

1.3.1 Ideal Fluid

If viscosity effect is negligible then the fluid is called ideal.

1.3.2 Real Fluid

All the fluids for which viscosity is not equal to zero i.e. $\mu \neq 0$ are called real fluids. These fluids may be compressible or incompressible.

1.3.3 Newtonian Fluids

Fluid obeying Newton's law of viscosity and for which μ has a constant value are known as Newtonian fluids. Mathematically

$$\tau = \mu \frac{du}{dy}. \tag{1.3.1}$$

Here τ is shear stress, $\frac{du}{dy}$ is shear strain rate and μ is the dynamic viscosity of the fluid.

1.4 Law of Conservation of Mass (Continuity Equation)

Consider a fixed volume in space (see Figure). The rate of increase of mass inside the volume

$$\frac{d}{dt}\int_v \rho dV = \int_v \frac{\partial \rho}{\partial t} dV, \tag{1.4.1}$$

where V is the volume. Since the volume is fixed, so $\frac{d}{dt}$ can be taken inside the integral. The rate of mass flow out of the volume is surface integral

$$\int_A \rho V.dA. \tag{1.4.2}$$

Here $\rho V.dA$ is the outward flux, because of the positive sign. By the law of conservation of mass "rate of increase of mass within a fixed volume must be equal to the rate of inflow through the boundaries", i.e.

$$\int_v \frac{\partial \rho}{\partial t} dV = -\int_A \rho V.dA. \tag{1.4.3}$$

By divergence theorem surface integral can be transformed into volume integral and so

$$\int_A \rho V.dA = \int_v \nabla.(\rho V) dV. \tag{1.4.4}$$

From Eqs. (1.5.3) and (1.5.4), we have

$$\int_v [\frac{\partial \rho}{\partial t} + \nabla.(\rho V)] dV = 0 \tag{1.4.5}$$

This relation holds for any volume, which is possible when integrand must vanish. This requires

$$\frac{\partial \rho}{\partial t} + \nabla.(\rho V) = 0 \tag{1.4.6}$$

which is called continuity equation.

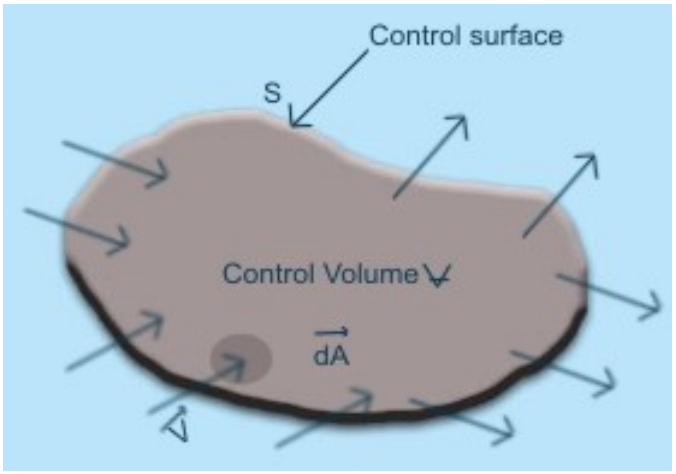

1.5 Different Forms of Continuity Equation

1.5.1 Steady Flow

For steady flow continuity equation becomes

$$\nabla.(\rho\mathbf{V}) = 0. \tag{1.5.1}$$

1.5.2 Incompressible Flow

For incompressible fluid, ρ is constant so

$$\frac{\partial\rho}{\partial t} = 0, \tag{1.5.2}$$

so equation of continuity becomes,

$$\nabla.(\rho\mathbf{V}) = 0, \tag{1.5.3}$$

as ρ is constant so above equation becomes

$$\rho(\nabla.\mathbf{V}) = 0, \tag{1.5.4}$$

and $\rho \neq 0$ so

$$(\nabla.\mathbf{V}) = 0. \tag{1.5.5}$$

1.6 Law of Conservation of Momentum

The law of conservation of momentum states that the total linear momentum of an isolated system remains constant regardless of changes within the system. In vector form, it can be written as

$$\rho\frac{d\mathbf{V}}{dt} = \nabla.\mathbf{T} + \rho\mathbf{b} \tag{1.6.1}$$

Where $\mathbf{V}$ is the velocity field, $\rho\mathbf{b}$ is the body force and $\mathbf{T}$ is the stress tensor.

1.7 Navier-Stokes Equation

In the component form the Navier-Stokes equation is

$$\rho\frac{Du_i}{Dt} = -\frac{\partial\rho}{\partial x_i} + \rho g_i + \frac{\partial}{\partial x_j}[2\mu e_{ij} - \frac{2}{3}\mu(\nabla.\mathbf{V})\delta_{ij}], \tag{1.7.1}$$

where p is the hydrostatic pressure, g is the gravity, μ is the dynamic viscosity and δ_{ij} is the Kronecker delta, defined by

$$\delta_{ij} = \begin{cases} 1 \quad , & \text{if } \ i = j \\ 0 \quad , & \text{if } i \neq j \end{cases} \tag{1.7.2}$$

and

$$e_{ij} = \frac{1}{2}(\frac{\partial u_i}{\partial x_j} + \frac{\partial u_j}{\partial x_i}), \tag{1.7.3}$$

if temperature differences are small within the fluid, then μ can be taken outside and Eq. (1.8.1) takes the form

$$\rho\frac{Du_i}{Dt} = -\frac{\partial\rho}{\partial x_i} + \rho g_i + 2\mu\frac{\partial e_{ij}}{\partial x_j} - \frac{2}{3}\mu\frac{\partial}{\partial x_i}(\nabla.\mathbf{V}), \tag{1.7.4}$$

$$= -\frac{\partial\rho}{\partial x_i} + \rho g_i + \mu[\nabla^2 u_i + \frac{1}{3}\frac{\partial}{\partial x_i}(\nabla.\mathbf{V})], \tag{1.7.5}$$

where

$$\nabla^2 u_i = \frac{\partial^2 u_i}{\partial x_j \partial x_i} = \frac{\partial^2 u_i}{\partial x_1^2} + \frac{\partial^2 u_i}{\partial x_2^2} + \frac{\partial^2 u_i}{\partial x_3^2}, \tag{1.7.6}$$

is Laplacian of u_i. For incompressible fluids $\nabla.\mathbf{V} = 0$ and using vector notation, the Navier-Stokes equation is

$$\rho\frac{D\mathbf{V}}{Dt} = -\nabla P + \rho\mathbf{g} + \mu\nabla^2\mathbf{V}. \tag{1.7.7}$$

This equation is valid only for incompressible fluid. If viscous effects are negligible then

$$\rho\frac{D\mathbf{V}}{Dt} = -\nabla P + \rho\mathbf{g} \tag{1.7.8}$$

which are the Euler equations of motion.

1.8 Some Common Useful Non-Dimensional Parameters

1.8.1 Reynolds Number

The Reynolds number is the fraction of inertia force to viscous force. Mathematically, it can be expressed as

$$Re = \frac{\text{inertial force}}{\text{viscous force}}. \tag{1.8.1}$$

1.8.2 Prandtl Number

Prandtl number is the ratio of momentum diffusitivity to heat diffusitivity. Mathematically

$$Pr = \frac{\text{momentum diffusitivity}}{\text{heat diffusitivity}} = \frac{\nu}{\alpha} = \frac{c_p \mu}{k}, \tag{1.8.2}$$

where

α = thermal diffusivity = $\frac{k}{\rho c_p}$

μ = dynamic viscosity

k = thermal conductivity

c_p = specific heat constant

ρ = density.

1.8.3 Eckert Number

The Eckert number expresses the relationship between the flows kinetic energy and enthalpy. Mathematically

$$E_c = \frac{V^2}{c_p \Delta T} = \frac{\text{kinetic energy}}{\text{enthalpy}}, \tag{1.8.3}$$

where

V = characteristic velocity of flow

c_p= specific heat constant

ΔT = characteristic temperature.

1.8.4 Nusselt Number

The ratio of convective to conductive heat transfer is called Nusselt number. Mathematically

$$Nu_L = \frac{hL}{k} = \frac{\text{convective heat transfer}}{\text{conductive heat transfer}}, \tag{1.8.4}$$

where

L = characteristic length

k = thermal conductivity of fluid

h = convective heat transfer coefficient of the fluid.

1.8.5 Sherwood Number

The ratio of convective to diffusive mass transfer is called Sherwood number. Mathematically

$$Sh = \frac{KL}{D} = \frac{\text{convective mass transfer coefficient}}{\text{diffusive mass transfer coefficient}}, \tag{1.8.5}$$

where

K = mass transfer coefficient

L = characteristic length

D = mass diffusitivity

1.9 Laws of Thermodynamics

1.9.1 First Law of Thermodynamics

This law states that, the increase in the internal energy of a system is equal to the amount of heat energy added to the system and work done by the system i.e.

$$\Delta e = W + Q \tag{1.9.1}$$

where e is the internal energy, W is the work done and Q is the amount of heat.

1.9.2 Second Law of Thermodynamics

Any thermodynamic process that proceeds from one equilibrium state to another, the entropy of the system plus environment remains unchanged or increase.

1.9.3 Third Law of Thermodynamics

As temperature approaches towards absolute zero, the entropy of a system approaches a constant.

1.10 Boundary Layer

A boundary layer is the layer of fluid in the immediate vicinity of a bounding surface where the effects of viscosity are significant.

1.11 Thermal Boundary Layer

The layer of a liquid or gaseous heat-transfer agent between the free stream and a heat-exchange surface. In this layer the temperature of the heat-transfer agent changes from that of the wall to that of the free stream.

1.12 Numerical Techniques

1.12.1 Shooting Method for Non-Linear Differential Equation

We explain shooting method for the following second order ODE

$$y'' = f(x, y, y'), \qquad a \leq x \leq b \tag{1.12.1}$$

with boundary conditions,

$$y(a) = C_1, \qquad y(b) = C_2. \tag{1.12.2}$$

The first step in shooting method is to reduce the bvp into the IVP.

$$y'' = f(x, y, y') \qquad \text{for} \qquad a \leq x \leq b$$

with

$$\text{y(a)} = C_1, \qquad y'(a) = s \text{ (unknown)}$$

In above equation s is unknown which needs to be find.

$$\lim_{t \longrightarrow \infty} y(b, s_t) = y(b) = C_2. \tag{1.12.3}$$

We generate a sequence of s_1, s_2,..... with s_o as the initial guess.
The iteration must stop when

$$y(b, s) - C_2 = 0 \tag{1.12.4}$$

This is a nonlinear equation in variable s. We use the Newton-Raphson method to generate the sequence s_t. In Newton's method only initial guess s_o required and generate the remaining terms by

$$s_t = s_{t-1} - \frac{(y(b, s_{t-1}) - C_2)}{\frac{dy}{ds}(b, s_{t-1})} \tag{1.12.5}$$

For two or more variable the Newton-Raphson formula is

$$s_t = s_{t-1} - \frac{(y(b, s_{t-1}) - C_2)}{|J|} \tag{1.12.6}$$

where J is the Jacobian matrix.

1.12.2 bvp4c

Boundary value problems (BVP) for ordinary differential equations (ODE) can be solved by using MATLAB bvp4c solver. The solver uses collocation method. It starts solution with an initial guess supplied at an initial mesh points and changes step-size (hence changes mesh) to get the specified accuracy. For more detail see reference [11].

Chapter 2

Numerical Solution of Stagnation-Point Flow of Nanofluid with Thermal Radiation Effect

This chapter is organized as follows.
In section 2.1 the introduction is given. In sections 2.2 and 2.3 we formulated the problem and the governing equations are presented. In section 2.4 we analyze the numerical results with the help of graphs and tables.

2.1 Introduction

This chapter review the work of Mustafa et al [7]. This chapter describes the MHD stagnation-point flow and heat transfer of nanofluid over a stretching sheet in the presence of thermal radiation. Strictly different application of Rosseland approximation for thermal radiation is made. The governing par-

tial differential equations are reduced into ordinary differential equations by similarity transformation. Then these equations have been solved by shooting method with fifth order Runge-Kutta integration technique. The solution have been validated with the built-in solver *bvp4c* of MATLAB. Graphs are included for the influence of different parameters on the flow field.

2.2 Problem Formulation

In this section we formulate the two-dimensional incompressible flow of nanofluid over a stretching sheet. The stretching sheet is placed at $y = 0$. Let us consider the velocities of stretching sheet $U_w = ax$ and the free stream $U_\infty = bx$, where $a, b > 0$. We consider the sheet at constant temperature T_w and nanoparticle concentration C_w. Ambient temperature and concentration are denoted by T_∞ and C_∞. The magnetic field is applied perpendicular to the flow with strength H_o. The boundary layer governing equations of nanofluids are

$$\frac{\partial u}{\partial x} + \frac{\partial v}{\partial y} = 0, \tag{2.2.1}$$

$$u\frac{\partial u}{\partial x} + v\frac{\partial u}{\partial y} = u_\infty \frac{du_\infty}{dx} + \nu_f \frac{\partial^2 u}{\partial y^2} - \frac{\sigma_e H_0^2}{\rho_f}(u - u_\infty), \tag{2.2.2}$$

where u and v are the components of velocity in x and y direction, ν_f is the kinematic viscosity, σ_e is the electrical conductivity, H_o is uniform magnetic field. The boundary conditions for the governing problem are

$$u = U_w(x) = ax, \qquad v = 0, \qquad \text{at} \qquad y = 0 \tag{2.2.3}$$

$$u \longrightarrow U_\infty(x) = bx, \qquad \text{as} \qquad y \longrightarrow \infty \tag{2.2.4}$$

Using the following dimensionless variables

$$\eta = \sqrt{\frac{a}{\nu_f}}y, \quad u = axf'(\eta) \quad , \quad v = -\sqrt{\nu_f}af(\eta), \tag{2.2.5}$$

$$\frac{\partial u}{\partial x} = af'(\eta) \quad , \quad u\frac{\partial u}{\partial x} = a^2xf'^2(\eta), \tag{2.2.6}$$

$$\frac{\partial u}{\partial y} = -axf''(\eta)\sqrt{\frac{a}{\nu_f}} \quad , \quad v\frac{\partial u}{\partial y} = -a^2xf''(\eta)f(\eta), \tag{2.2.7}$$

$$\frac{\partial u_\infty}{\partial x} = b \quad , \quad u_\infty\frac{\partial u_\infty}{\partial x} = b^2x, \tag{2.2.8}$$

where

$$\frac{\partial^2 u}{\partial y^2} = -axf'''(\eta)\frac{a}{\nu_f} \quad , \quad \nu_f\frac{\partial^2 u}{\partial y^2} = -a^2xf'''(\eta), \tag{2.2.9}$$

$$\frac{\sigma_e H_o^2}{\rho_f}(u - u_\infty) = aM(axf'(\eta) - bx), \tag{2.2.10}$$

$$\frac{\partial v}{\partial y} = -af'(\eta). \tag{2.2.11}$$

Insert Eq. (2.2.6) and Eq. (2.2.11) in Eq. (2.2.1) we get

$$af'(\eta) - af'(\eta) = 0.$$

Therefore, Eq. (2.2.1) is identically satisfied. Now, we put Eqs. (2.2.6) to (2.2.10) in Eq. (2.2.2) we get

$$a^2xf'^2(\eta) - a^2xf''(\eta)f(\eta) = b^2x + a^2xf'''(\eta) - aM(axf'(\eta) - bx), \tag{2.2.12}$$

after simplifying the above Eq. (2.2.12) we obtain

$$f''' + ff'' - f'^2 + \lambda^2 + M(\lambda - f') = 0. \tag{2.2.13}$$

In the final step we convert boundary conditions into the new variable.

when $\eta = 0$ then

$$u = axf'(0), \tag{2.2.14}$$

by comparing Eq. (2.2.3) and Eq. (2.2.14) we obtain

$$\begin{aligned} ax &= axf'(0), \\ f'(0) &= 1. \end{aligned} \tag{2.2.15}$$

when $\eta = 0$ then

$$v = -\sqrt{\nu_f a} f(0) \tag{2.2.16}$$

By equating Eq. (2.2.3) and Eq. (2.2.16) we get

$$f(0) = 0. \tag{2.2.17}$$

Comparing both values of u when $y \longrightarrow \infty$ and $\eta \longrightarrow \infty$

$$\begin{aligned} x &= axf'(\infty), \\ \frac{b}{a} &= f'(\infty), \\ f'(\infty) &= \lambda, \end{aligned} \tag{2.2.18}$$

where $M = \frac{\sigma H_o}{\rho f a}$ is a magnetic parameter and $\lambda = \frac{b}{a}$ is the ratio of the free stream velocity to the velocity of the stretching sheet.

2.3 Transport Equations

The governing equations of energy and nanoparticles concentration are given by

$$\begin{aligned} u\frac{\partial T}{\partial x} + v\frac{\partial T}{\partial y} = \alpha\frac{\partial^2 T}{\partial y^2} + \frac{\nu_f}{C_f}(\frac{\partial u}{\partial y})^2 - \frac{1}{(\rho C)_f}(\frac{\partial q_r}{\partial y}) + \\ \frac{\sigma_e H_0^2}{(\rho C)_f}(u_\infty - u)^2 + \tau[D_B\frac{\partial T}{\partial y}\frac{\partial C}{\partial y} + \frac{D_T}{T_\infty}(\frac{\partial T}{\partial y})^2], \end{aligned} \tag{2.3.1}$$

$$u\frac{\partial C}{\partial x} + \frac{v\partial C}{\partial y} = D_B\frac{\partial^2 C}{\partial y^2} + \frac{D_T}{T_\infty}\frac{\partial^2 T}{\partial y^2}, \tag{2.3.2}$$

In above equations T= temperature

C = nanoparticles concentration

α = thermal diffusivity

C_f = specific heat constant of fluid

D_B = Brownian motion coefficient

D_T = thermophoretic diffusion coefficient

τ = ratio of effective heat capacity of the nanoparticles to the heat capacity of fluid

q_r= radiative heat flux.

$$q_r = -\frac{4\sigma^*}{3k^*}\frac{\partial T^4}{\partial y} = -\frac{16\sigma^*}{3k^*}T^3\frac{\partial T}{\partial y}, \tag{2.3.3}$$

where σ^* and k^* are the Stefan-Boltzman constant and the mean absorption coefficient, respectively. Now Eq. (2.3.1) can be expressed as

$$u\frac{\partial T}{\partial x} + v\frac{\partial T}{\partial y} = \frac{\partial}{\partial y}[(\alpha + \frac{16\sigma^* T^3}{3\rho C_p k^*})\frac{\partial T}{\partial y}] + \frac{\nu_f}{C_p}(\frac{\partial u}{\partial y})^2 + \frac{\sigma_e H_0^2}{(\rho C)_f}(u_\infty - u)^2 + \tau[D_B\frac{\partial T}{\partial y}\frac{\partial C}{\partial y} + \frac{D_T}{T_\infty}(\frac{\partial T}{\partial y})^2]. \tag{2.3.4}$$

2.3.1 Constant Wall Temperature (CWT)

The relevant boundary condition in this situation are

$$T = T_w, \quad C = C_w, \quad at \quad y = 0, \tag{2.3.5}$$

$$T \longrightarrow T_\infty, \quad C \longrightarrow C_\infty, \quad as \quad y \longrightarrow \infty. \tag{2.3.6}$$

We now define the non-dimensional $\theta(\eta) = \frac{T-T_\infty}{T_w-T_\infty}$ with $T = T_\infty(1+(\theta_w-1)\theta)$ and $\theta_w = \frac{T_w}{T_\infty}$ (temperature parameter), and the non-dimensional concentration $\phi_\eta = \frac{C-C_\infty}{C_w-C_\infty}$. The first term on the right hand side of Eq. (2.3.4) can be written as

$$\alpha\frac{\partial}{\partial y}[\frac{\partial T}{\partial y}(1 + R_d(1 + \theta_w - 1)\theta)^3],$$

where $R_d = \frac{16\sigma^* T_\infty^3}{3kk^*}$ denotes the radiation parameter for the CWT case, and R_d provides no thermal radiation effect.

First we convert Eq. (2.3.4) into ODEs,

$$\begin{aligned} T &= T_\infty(1 + (\theta_w - 1)\theta), \\ T &= (T_w - T_\infty)\theta(\eta) + T_\infty, \qquad (2.3.7) \\ C &= (C_w - C_\infty)\phi(\eta) + C_\infty, \qquad (2.3.8) \\ u\frac{\partial T}{\partial x} &= 0, \qquad (2.3.9) \\ \frac{\partial T}{\partial y} &= (T_w - T_\infty)\theta'(\eta)\sqrt{\frac{a}{\nu_f}}, \\ v\frac{\partial T}{\partial y} &= -a(T_w - T_\infty)f(\eta)\theta'(\eta), \qquad (2.3.10) \end{aligned}$$

$$\frac{\partial}{\partial y}[(\alpha + \frac{16\sigma^* T^3}{3\rho c_p k^*})\frac{\partial T}{\partial y}] = \alpha\frac{\partial}{\partial y}[(1 + \frac{16\sigma^* T^3}{3\rho c_p k^* \alpha}) \quad (T_w - T_\infty) \theta'(\eta)\sqrt{\frac{a}{\nu_f}}]. \qquad (2.3.11)$$

As we know that $\alpha = \frac{k}{\rho c_p}$ after putting this value in Eq. (2.3.11) we get

$$\begin{aligned} \frac{\partial}{\partial y}[(\alpha + \frac{16\sigma^* T^3}{3\rho c_p k^*})\frac{\partial T}{\partial y}] &= \alpha\frac{a}{\nu_f}(T_w - T_\infty)[1 + R_d(1 + (\theta_w - 1)\theta)^3\theta'(\eta)]', \\ = \frac{a}{P_r}(T_w &- T_\infty)[1 + R_d(1 + (\theta_w - 1)\theta)^3\theta'(\eta)]', \qquad (2.3.12) \\ \frac{\nu_f}{c_p}\frac{\partial u}{\partial y} &= axf''(\eta)\sqrt{\frac{a}{\nu_f}}, \qquad (2.3.13) \\ \frac{\nu_f}{c_p}(\frac{\partial u}{\partial y})^2 &= \frac{a^3x^2}{c_p}f''^2(\eta), \qquad (2.3.14) \\ \frac{\sigma_e H_0^2}{(\rho c)_f}(u_\infty - u)^2 &= \frac{\sigma_e H_0^2}{(\rho c)_f}(bx - axf'(\eta)), \qquad (2.3.15) \\ \tau D_B\frac{\partial T}{\partial y}\frac{\partial C}{\partial y} &= \tau D_B(T_w - T_\infty)(C_w - C_\infty)\frac{a}{\nu_f}\theta'(\eta)\phi'(\eta), \qquad (2.3.16) \\ \frac{D_T}{T_\infty}(\frac{\partial T}{\partial y})^2 &= (T_w - T_\infty)^2\theta'^2(\eta)\frac{a}{\nu_f}. \qquad (2.3.17) \end{aligned}$$

Insert above Eqs. in Eq. (2.3.4)

$$-a(T_w - T_\infty)f(\eta)\theta'(\eta) = \frac{a}{P_r}(T_w - T_\infty)[1 + R_d(1 + (\theta_w - 1)\theta)^3\theta'(\eta)]' + \frac{a^3x^2}{c_p}f''^2(\eta) + \frac{\sigma_e H_0^2}{(\rho c)_f}(bx - axf'(\eta))^2 + \tau D_B(T_w - T_\infty)(C_w - C_\infty) \frac{a}{\nu_f}\theta'(\eta)\phi'(\eta) + (T_w - T_\infty)^2\theta'^2(\eta)\frac{a}{\nu_f},$$

Dividing both sides by $-a(T_w - T_\infty)$

$$\frac{1}{P_r}[1 + R_d(1 + (\theta_w - 1)\theta)^3\theta'(\eta)]' + f(\eta)\theta'(\eta) + \frac{a^2x^2}{(T_w - T_\infty)c_p}f''^2(\eta) + \frac{\sigma_e H_0^2 a^2x^2}{(\rho c)_f a(T_w - T_\infty)} (\lambda - f'(\eta))^2 + \frac{\tau D_B(C_w - C_\infty)}{v_f}\phi'(\eta)\theta'(\eta) + \frac{\tau D_T(T_w - T_\infty)}{T_\infty v_f}\theta'^2 = 0,$$

As we know that $ax = u_w$. So above equation becomes

$$\frac{1}{P_r}[1 + R_d(1 + (\theta_w - 1)\theta)^3\theta'(\eta)]' + f(\eta)\theta'(\eta) + N_b\phi'(\eta)\theta'(\eta) + N_t\theta'^2 + E_c^* f''^2(\eta) + ME_c^*(\lambda - f'(\eta))^2 = 0. \quad (2.3.18)$$

Now we convert Eq. (2.3.2) into ODE

$$u\frac{\partial C}{\partial x} = 0, \quad (2.3.19)$$

$$\frac{\partial C}{\partial y} = (C_w - C_\infty)\phi'(\eta)\sqrt{\frac{a}{v_f}},$$

$$v\frac{\partial C}{\partial y} = -a(C_w - C_\infty)\phi'(\eta)f(\eta), \quad (2.3.20)$$

$$D_B\frac{\partial^2 C}{\partial y^2} = \frac{aD_B}{v_f}(C_w - C_\infty)\phi''(\eta), \quad (2.3.21)$$

$$\frac{D_T}{T_\infty}\frac{\partial^2 T}{\partial y^2} = \frac{aD_T}{v_f T_\infty}(T_w - T_\infty)\theta''(\eta). \quad (2.3.22)$$

After putting Eqs. (2.3.19) to (2.3.22) in Eq. (2.3.2) we get

$$-a(C_w - C_\infty)\phi'(\eta)f(\eta) = \frac{aD_B}{v_f}(C_w - C_\infty)\phi''(\eta) + \frac{aD_T}{v_f T_\infty}(T_w - T_\infty)\theta''(\eta).$$

Dividing both sides of above equation by $\frac{aD_B}{v_f}(C_w - C_\infty)$

$$\phi''(\eta) + L_e\phi'(\eta)f(\eta) + \frac{N_t}{N_b}\theta''(\eta) = 0. \quad (2.3.23)$$

Now we convert the boundary conditions into the new form.

$$T = T_w, \qquad C = C_w, \qquad at \qquad y = 0$$
$$T \longrightarrow \infty, \qquad C \longrightarrow \infty, \qquad as \qquad y \longrightarrow \infty.$$

When y=0 then T is

$$T = T_w,$$

and when $\eta = 0$ then T is

$$T = (T_w - T_\infty)\ \theta(0) + T_\infty,$$

comparing values of T at $y = 0$ and $\eta = 0$

$$T_w = (T_w - T_\infty)\ \theta(0) + T_\infty,$$
$$\theta(0) = 1.$$

When y=0 then C is

$$C = C_w,$$

and when $\eta = 0$ then C is

$$C = (C_w - C_\infty)\ \phi(0) + C_\infty,$$

comparing values of C at $y = 0$ and $\eta = 0$

$$C_w = (C_w - C_\infty)\ \phi(0) + C_\infty,$$
$$\phi(0) = 1.$$

When $y \longrightarrow \infty$ then T is

$$T = T_\infty,$$

and when $\eta \longrightarrow \infty$ then T is

$$T = (T_w - T_\infty)\theta(\infty) + T_\infty,$$

comparing values of T when $y \longrightarrow \infty$ and $\eta \longrightarrow \infty$

$$T_\infty = (T_w - T_\infty)\theta(\infty) + T_\infty,$$
$$\theta(\infty) = 0.$$

When $y \longrightarrow \infty$ then C becomes

$$C = C_\infty,$$

and when $\eta = 0$ then C becomes

$$C = (C_w - C_\infty)\phi(\infty) + C_\infty,$$

comparison of C at $y \longrightarrow \infty$ and $\eta \longrightarrow \infty$

$$C_\infty = (C_w - C_\infty)\phi(\infty) + C_\infty,$$
$$\phi(\infty) = 0.$$

So relevant boundary condition with respect to ODEs in CWT case are

$$\theta(0) = 1, \qquad \phi(0) = 1 \qquad at \qquad \eta = 0 \tag{2.3.24}$$

$$\theta(\eta) = 0, \qquad \phi(\eta) = 0 \qquad as \qquad \eta \to \infty, \tag{2.3.25}$$

where $N_b = \frac{\tau D_B(C_w - C_\infty)}{v_f}$, $N_t = \frac{\tau D_T(T_w - T_\infty)}{T_\infty v_f}$ are the Brownian and thermophoretic constants respectively and $E_c^* = \frac{U_w^2}{C_p(T_w - T_\infty)}$ is the local Eckert number. We look for the availability of local similarity solutions. The surface heat and mass fluxes are defined by the following equations

$$q_w = -k(\frac{\partial T}{\partial y})_{y=0} + (q_r)_w = -k(T_w - T_\infty)\sqrt{\frac{a}{\nu}}[1 + R_d\theta_w^3]\theta_0',$$

and

$$j_w = -D_B(\frac{\partial C}{\partial y})_{y=0} = -D_B(C_w - C_\infty)\sqrt{\frac{a}{\nu}}\phi_0',$$

with the help of local Nusselt number $Nu_x = \frac{xq_w}{k(T_w - T_\infty)}$ and local Sherwood number Sh $= \frac{xj - w}{D_B(c_w - c_\infty)}$ one obtains $\frac{Nu_x}{\sqrt{Re}_x} = -[1 + R_d\theta_w^3]\theta'(0) = Nu_r$, $\frac{Sh}{\sqrt{Re}_x} = -\phi(0)$ =Shr.

2.3.2 Prescribed Surface Temperature (PST)

The boundary conditions in this case are

$$T = T_w = T_\infty + cx^2, \quad C = C_w = C_\infty + dx^2, \quad at \quad y = 0, \tag{2.3.26}$$

$$T \longrightarrow T_\infty, \qquad C \longrightarrow C_\infty, \qquad as \quad y \longrightarrow \infty, \tag{2.3.27}$$

where c, d> 0 are constants. Defining the dimensionless temperature $\theta(\eta) = \frac{T-T_\infty}{T_w-T_\infty}$ and nanoparticles concentration $\phi(\eta) = \frac{C-C_\infty}{C_w-C_\infty}$.
Now, we convert Eq. (2.3.2) and Eq. (2.3.4) into ODEs.
First, we assume that the temperature difference within the flow such as that the term T^4 may be expressed as a linear function of temperature. Hence, expanding T^4 in a Taylor series about T_∞ and neglecting higher order terms we get

$$T^4 = 4T_\infty^3 T - 3T_\infty^4,$$

we have

$$-\frac{1}{\rho c_p}\frac{\partial q_r}{\partial y} = \frac{16\sigma^* T_\infty^3}{3\rho c_p k^*}\frac{\partial^2 T}{\partial y^2}.$$

After simplifying the first term of Eq. (2.3.4) becomes

$$\alpha(1 + R_d)\tfrac{\partial^2 T}{\partial y^2},$$

where

$$R_d = \tfrac{16\sigma^* T_\infty^3}{3kk^*}.$$

In view of above calculation Eq. (2.3.4) becomes

$$u\frac{\partial T}{\partial x} + v\frac{\partial T}{\partial y} = \alpha(1 + R_d)\frac{\partial^2 T}{\partial y^2} + \frac{\nu_f}{C_p}(\frac{\partial u}{\partial y})^2 + \frac{\sigma_e H_0^2}{(\rho C)_f}$$
$$(u_\infty - u)^2 + \tau D_B[\frac{\partial T}{\partial y}\frac{\partial C}{\partial y} + \frac{D_T}{T_\infty}(\frac{\partial T}{\partial y})^2]. \tag{2.3.28}$$

As given that

$$\begin{aligned} T &= T_w = T_\infty + cx^2, \\ T &= T_w - T_\infty = cx^2, \\ T &= cx^2\theta(\eta) + T_\infty, \qquad (2.3.29) \\ \frac{\partial T}{\partial x} &= 2cx\theta(\eta), \\ u\frac{\partial T}{\partial x} &= 2acx^2 f'(\eta)\theta(\eta). \qquad (2.3.30) \end{aligned}$$

By using $T = T_w - T_\infty = cx^2$ in Eq. (2.3.30), we have

$$\begin{aligned} u\frac{\partial T}{\partial x} &= 2a(T_w - T_\infty)f'(\eta)\theta(\eta), \qquad (2.3.31) \\ \frac{\partial T}{\partial y} &= (T_w - T_\infty)\sqrt{\frac{a}{\nu_f}}, \\ v\frac{\partial T}{\partial y} &= -a(T_w - T_\infty)\theta'(\eta)f(\eta), \qquad (2.3.32) \\ \alpha(1+R_d)\frac{\partial^2 T}{\partial y^2} &= \frac{a\alpha(1+R_d)(T_w - T_\infty)\theta''(\eta)}{\nu_f}, \qquad (2.3.33) \\ \frac{\nu_f}{c_p}(\frac{\partial u}{\partial y})^2 &= \frac{\nu a^3 x^2 f''^2(\eta)}{c_p \nu_f}, \qquad (2.3.34) \\ \frac{\sigma_e H_0^2}{\rho c_p}(bx - axf'(\eta))^2 &= \frac{\sigma_e a^2 x^2 H_0^2}{\rho c_p}(\lambda - f'^2\eta), \qquad (2.3.35) \\ \tau D_B \frac{\partial T}{\partial y}\frac{\partial C}{\partial y} &= (T_w - T_\infty)(C_w - C_\infty)\theta'(\eta)\phi'(\eta)\frac{a}{\nu_f}, \qquad (2.3.36) \\ \frac{\tau D_T}{T_\infty}(\frac{\partial T}{\partial y})^2 &= \frac{a\tau D_T (T_w - T_\infty)^2 \theta'^2(\eta)}{T_\infty \nu_f}. \qquad (2.3.37) \end{aligned}$$

Insert Eqs. (2.3.31) to (2.3.37) in Eq. (2.3.28) we obtain

$$\begin{aligned} 2a(T_w - T_\infty)f'(\eta)\theta(\eta) - a(T_w - T_\infty)\theta'(\eta)f(\eta) &= \frac{a\alpha(1+R_d)(T_w - T_\infty)\theta''(\eta)}{\nu_f} \\ + \frac{\nu a^3 x^2 f''^2(\eta)}{c_p \nu_f} + \frac{\sigma_e a^2 x^2 H_0^2}{\rho c_p}(\lambda - f'\eta)^2 + (T_w - T_\infty)(C_w - C_\infty)\theta'(\eta)\phi'(\eta)\frac{a}{\nu_f} \\ + \frac{a\tau D_T (T_w - T_\infty)^2 \theta'^2(/eta)}{T_\infty \nu_f}. \end{aligned}$$

Dividing both sides of above Eq. by $-a(T_w - T_\infty)$

$$2f'(\eta)\theta(\eta) - \theta'(\eta)f(\eta) = \frac{(1+R_d)\theta''(\eta)}{P_r} + \frac{\nu a^2 x^2 f'''^2(\eta)}{c_p \nu_f (T_w - T_\infty)} + \frac{\sigma_e a^2 x^2 H_0^2}{a(T_w - T_\infty)\rho c_p}$$
$$(\lambda - f'(\eta))^2 + \frac{\tau D_B (C_w - C_\infty)\theta'(\eta)\phi'(\eta)}{\nu_f} + \frac{\tau D_T (T_w - T_\infty)\theta'^2(/eta)}{T_\infty \nu_f},$$

now put $a^2x^2 = u_w^2$ in above equation

$$2f'(\eta)\theta(\eta) - \theta'(\eta)f(\eta) = \frac{(1+R_d)\theta''(\eta)}{P_r} + \frac{\nu u_w^2 f'''^2(\eta)}{c_p \nu_f (T_w - T_\infty)} + \frac{\sigma_e u_w^2 H_0^2}{a(T_w - T_\infty)\rho c_p}$$
$$(\lambda - f'(\eta))^2 + \frac{\tau D_B (C_w - C_\infty)\theta'(\eta)\phi'(\eta)}{\nu_f} + \frac{\tau D_T (T_w - T_\infty)\theta'^2(\eta)}{T_\infty \nu_f},$$

where $M = \frac{\sigma H_0}{\rho f a}$ is a magnetic parameter, $\lambda = \frac{b}{a}$ is the ratio of the free stream velocity, $N_b = \frac{\tau D_B (C_w - C_\infty)}{v_f}$, $N_t = \frac{\tau D_T (T_w - T_\infty)}{T_\infty v_f}$ are the Brownian and thermophoretic constants respectively and $E_c^* = \frac{U_w^2}{C_p (T_w - T_\infty)}$ is the local Eckert number. After putting all these values in above equation, it becomes

$$\frac{(1+R_d)}{P_r}\theta''(\eta) + \quad f(\eta)\theta'(\eta) - 2f'(\eta)\theta(\eta) + N_b\theta'(\eta)\phi'(\eta) + N_t\theta'^2(\eta)$$
$$+E_c f'''^2(\eta) + ME_c(\lambda - f'(\eta))^2 = 0. \qquad (2.3.38)$$

Now we convert Eq. (2.3.2) into ODE

As given that

$$\begin{aligned} C &= C_w = C_\infty + dx^2, \\ C &= C_w - C_\infty = dx^2, \\ C &= dx^2\phi(\eta) + C_\infty, \qquad (2.3.39) \\ \frac{\partial C}{\partial x} &= 2dx\phi(\eta), \\ u\frac{\partial C}{\partial x} &= 2adx^2 f'(\eta)\phi(\eta). \qquad (2.3.40) \end{aligned}$$

Use $C = C_w - C_\infty = dx^2$ in Eq. (2.3.40)

$$u\frac{\partial C}{\partial x} = 2a(C_w - C_\infty)f'(\eta)\phi(\eta), \tag{2.3.41}$$

$$v\frac{\partial C}{\partial y} = -a(C_w - C_\infty)f(\eta)\phi'(\eta), \tag{2.3.42}$$

$$D_B\frac{\partial^2 C}{\partial y^2} = \frac{aD_B(C_w - C_\infty)\phi''(\eta)}{\nu_f}, \tag{2.3.43}$$

$$\frac{D_T}{T_\infty}\frac{\partial^(2)T}{\partial y^2} = \frac{aD_T(T_w - T_\infty)\theta''(\eta)}{T_\infty\nu_f}. \tag{2.3.44}$$

Put Eqs. (2.3.41) to (2.3.44) in Eq. (2.3.2)

$$2a(C_w - C_\infty)f'(\eta)\phi(\eta) - a(C_w - C_\infty)f(\eta)\phi'(\eta) = \frac{aD_B(C_w - C_\infty)\phi''(\eta)}{\nu_f} + \frac{aD_T(T_w - T_\infty)\theta''(\eta)}{T_\infty\nu_f}.$$

Divide both sides of above Eq. by $\frac{aD_B(C_w - C_\infty)}{\nu_f}$,

$$\phi''(\eta) - 2\frac{\nu_f}{D_B}\phi(\eta)f'(\eta) + \frac{\nu_f}{D_B}\phi'(\eta)f(\eta) + \frac{1}{\frac{\tau D_B(C_w - C_\infty)}{\nu_f}}\frac{\tau D_T(T_w - T_\infty)}{\nu_f T_\infty}\theta''(\eta) = 0,$$

after simplifying it becomes

$$\phi''(\eta) + L_e[\phi'(\eta)f(\eta) - 2\phi(\eta)f'(\eta)] + \frac{N_t}{N_b}\theta''(\eta) = 0. \tag{2.3.45}$$

Now we convert boundary condition into the new form.

From Eqs. (2.3.24) and (2.3.25) we know that

$$T = T_w = T_\infty + cx^2, \quad C = C_w = C_\infty + dx^2 \quad at \quad y = 0,$$

$$T \longrightarrow T_\infty, \qquad C \longrightarrow C_\infty, \qquad as \quad y \longrightarrow \infty.$$

As we know

$$\eta = \sqrt{\frac{a}{\nu_f}}y,$$

so, when $y = 0$ then $\eta = 0$.

$$T = (T_w - T_\infty)\theta(\eta) + T_\infty, \tag{2.3.46}$$

$$C = (C_w - C_\infty)\phi(\eta) + C_\infty. \tag{2.3.47}$$

Put $\eta = 0$ in Eq. (2.3.46) and compare both values of T at $y = 0$ and $\eta = 0$

$$cx^2 + T_\infty = (T_w - T_\infty)\theta(0) + T_\infty,$$

As we know that $cx^2 = T_w - T_\infty$. So above equation becomes

$$\theta(0) = 1.$$

Put $\eta = 0$ in Eq. (2.3.47) and comparing both values of C at $y = 0$ and $\eta = 0$

$$dx^2 + C_\infty = (C_w - C_\infty)\phi(0) + C_\infty,$$

as we know that $dx^2 = (C_w - C_\infty)$. So above equation becomes

$$\phi(0) = 1.$$

Put $\eta = \infty$ in Eq. (2.3.46) and comparing both values of T at y=∞ and η=∞

$$T_\infty = (T_w - T_\infty)\theta(\infty) + T_\infty,$$

after simplifying

$$\theta(\infty) = 0.$$

Put η= ∞ in Eq. (2.3.47) and comparing both values of C at $y = \infty$ and η =∞

$$C_\infty = (C_w - C_\infty)\phi(\infty) + C_\infty,$$

after simplifying

$$\phi(\infty) = 0.$$

Here the heat and mass transfer rates at the sheet becomes

$$q_w = -k(\frac{\partial T}{\partial y})\partial\partial_{y=0} + (q_r)_w = -kcx^2\sqrt{\frac{a}{\nu}}[1 + R_d]\theta'(0),$$

and

$$j_w = -D_B(\frac{\partial C}{\partial y})_{y=0} = -D_B(C_w - C_\infty)\sqrt{\frac{a}{\nu}}\phi'(0),$$

using the definition of reduced Nusselt and Sherwood numbers one obtains

$$\frac{Nu_x}{\sqrt{Re_x}} = -[1 + R_d]\theta'(0) = Nur,$$

$$\frac{Sh}{\sqrt{Re_x}} = -\phi'(0) = Shr.$$

2.4 Numerical Results and Discussion

The numerical solution of governing differential systems for different values of thermophoretic parameter N_t, Brownian parameter N_b and thermal radiation parameter R_d is obtained using shooting method with fifth order Runge-Kutta integration technique. The resulting equations are first reduced to the first order equations and then apply shooting method to solve the problem. We have drawn Figs. 2.1-2.8 to examine the effects of different parameter and prepared Tables 1 and 2.

2.4.1 Heat and Mass Transfer Rates

In this subsection we discuss the behavior of $\theta'(0)$ and $\phi'(0)$ for different parametric values of N_b and N_t. Tables 1 and 2 gives the values in CWT and PST cases respectively. Heat and mass flux decreases from the sheet

when the radiation effect strengthens. This decrease is associated with the values of $\theta'(0)$ and $\phi'(0)$. The heat transfer rate decreases with an increase in Brownian motion parameter. The reduced sherwood number is increased due to increase in $-\phi(0)$ when N_b is increased. The effect of N_b on the Nur and Shr is similar for $R_d = 0$ and $R_d = 1$. For a fixed N_b there is decrease in magnitude of reduced Nusselt number with an increase in N_t. It is found that the values of $-\phi'(0)$ increases with an increase in thermophoretic constant with and without R_d. The outcomes also show that values of reduced Nusselt and Sherwood number in the PST case are significant when compared with the CWT case.

Table 1. Value of dimensionless heat transfer rate $-\theta'(0)$ and dimensionless mass transfer rate $-\phi'(0)$ for different values of the N_b, N_t and R_d when $\lambda = 0.5$, M = 0.5, Pr = 7, Le = 1, Ec = 0.2 in the CWT case.

N_b	N_t	R_d	$-\theta'(0)$ shooting method	$-\theta'(0)$ bvp4c	$-\phi'(0)$ shooting method	$-\phi'(0)$ bvp4c
0.1	0.1	0	1.26202	1.26202	-0.11439	-0.11440
		1	0.62939	0.62939	0.43257	0.43257
0.2		0	1.02577	1.02578	0.40213	0.40213
		1	0.57635	0.57635	0.58769	0.58769
0.3		0	0.81541	0.81543	0.56553	0.56552
		1	0.52643	0.52643	0.63842	0.63842
0.4		0	0.63142	0.63142	0.64056	0.64056
		1	0.47959	0.47959	0.66305	0.66305
0.1	0.1	0	1.26202	1.26203	-0.11439	-0.11440
		1	0.63180	0.62938	0.43257	0.43257
	0.2	0	1.08471	1.08473	-0.59564	-0.59569
		1	0.59155	0.59155	0.23152	0.23150
	0.3	0	0.92689	0.92691	-0.80536	-0.80540
		1	0.55582	0.55582	-0.11439	-0.11439
	0.4	0	0.78750	0.78750	-0.79755	-0.79755
		1	0.52212	0.52212	-0.00320	-0.00320

Table 2. Value of dimensionless heat transfer rate $-\theta'(0)$ and dimensionless mass transfer rate $-\phi'(0)$ for different values of the N_b, N_t and R_d when $\lambda = 0.5$, M = 0.5, Pr = 7, Le = 1, Ec = 0.2 in the PST case.

N_b	N_t	R_d	$-\theta'(0)$ shooting method	$-\theta'(0)$ bvp4c	$-\phi'(0)$ shooting method	$-\phi'(0)$ bvp4c
0.1	0.1	0	3.14763	3.14763	-0.72904	-0.72904
		1	2.36895	2.36895	-0.04391	-0.04391
0.2		0	2.77955	2.77954	0.55857	0.55857
		1	2.19423	2.19423	0.76836	0.76836
0.3		0	2.48849	2.48848	0.93008	0.93008
		1	2.02774	2.02773	1.04404	1.04404
0.4		0	2.21418	2.21416	1.12869	1.12869
		1	1.86606	1.86606	1.19349	1.19349
0.1	0.1	0	3.14763	3.14763	-0.72903	-0.72904
		1	2.36895	2.36895	-0.04391	-0.04391
	0.2	0	2.79704	2.79704	-2.02930	-2.02930
		1	2.23776	2.23776	-1.31297	-1.31297
	0.3	0	2.63806	2.63806	-3.66695	-3.66695
		1	2.10831	2.10831	-2.30700	-2.30700
	0.4	0	2.4350	2.4350	-4.6516	-4.6516
		1	2.0074	2.0074	-3.2810	-3.2810

2.4.2 Velocity Profile

The outcomes of velocity profile for different values of magnetic parameter M and velocity ratio λ are shown in Fig. 2.1. It can be seen from the Fig. 2.1 that by increasing λ ($\lambda > 1$) the velocity increases and boundary layer thickness decreases. Fig. 2.1 shows that for $\lambda < 1$ the flow has reversed boundary layer structure. In this case the boundary layer thickness increases due to decrease in the free stream velocity. Furthermore boundary layer thickness decreases with an increase in the magnetic parameter M. The Lorentz force increases by increasing M. This increase in Lorentz force reduce the velocity of fluid due to drag force.

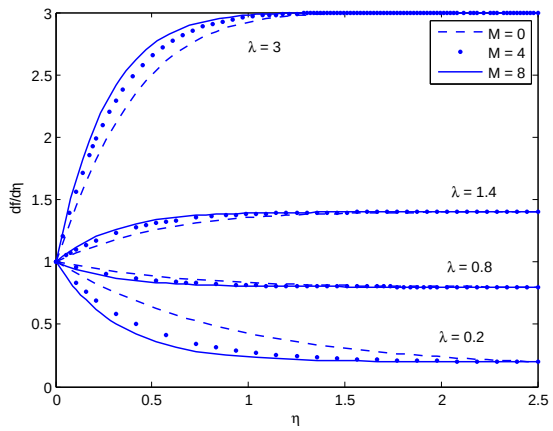

Figure 2.1: Influence of M and λ on f'

2.4.3 Temperature Profiles

The effects of Brownian motion parameter N_b are presented in Fig. 2.2. It is observed that the temperature and thermal boundary thickness increase by increasing N_b in both CWT and PST cases. The outcomes of thermophoretic effect are shown in Fig. 2.3. It is found that the temperature increases with increasing values of N_t. Fig. 2.4 displays the impact of thermal radiation parameter R_d on the temperature profile. From Fig. 2.4 it is seen that with the increase of R_d the temperature also increases. Fig. 2.5 plots the effect of Pr on the temperature. The temperature θ decreases rapidly near the boundary with an increase in Pr. Comparatively the influence of parameters on the temperature profile is bigger in CWT case than the PST case.

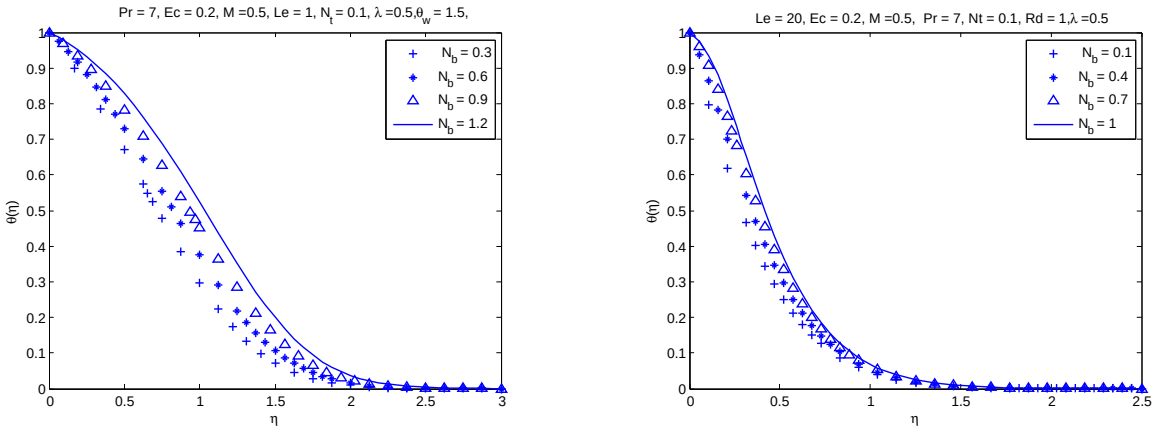

Figure 2.2: Influence of N_b on θ. (left CWT, right PST)

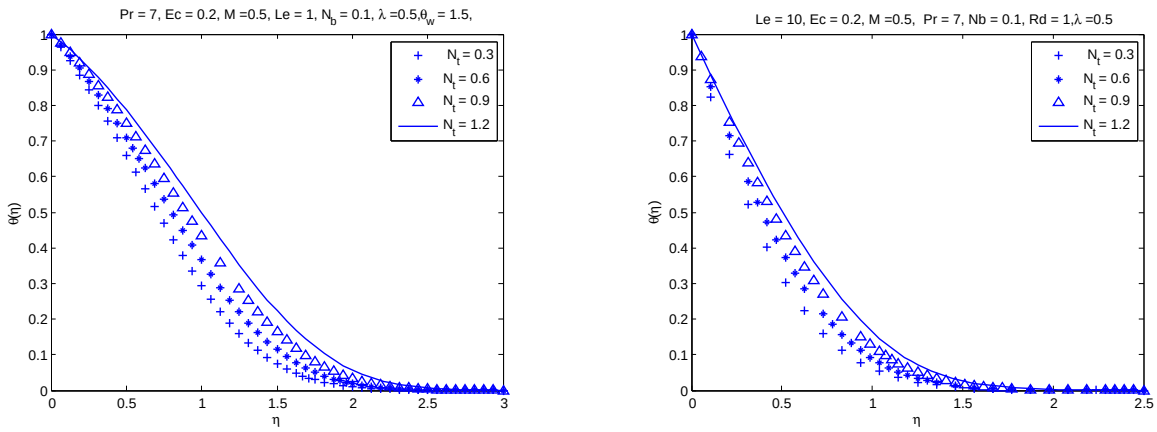

Figure 2.3: Influence of N_t on θ. (left CWT, right PST)

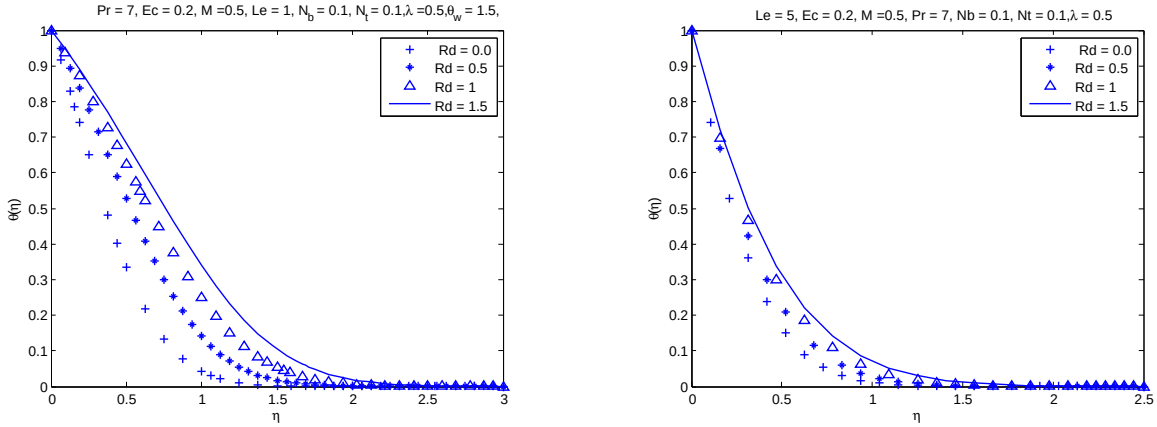

Figure 2.4: Influence of R_d on θ. (left CWT, right PST)

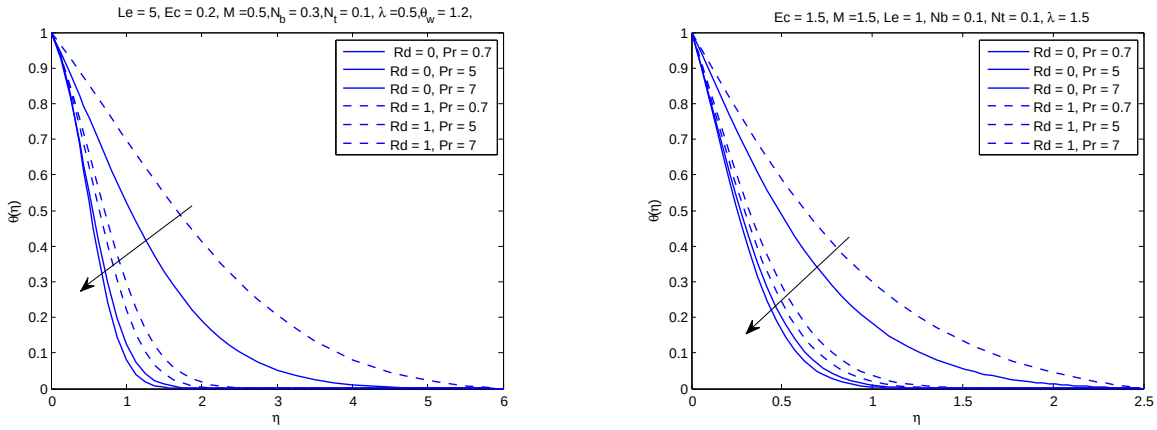

Figure 2.5: Influence of P_r on θ. (left CWT, right PST)

2.4.4 Nanoparticles Concentration Profiles

Fig. 2.6 illustrates the outcome of an increase in the Brownian motion parameter N_b on the nanoparticles profile ϕ. We observe that ϕ is increases by decreasing N_b. Fig. 2.7 is plotted to analyze the effects of thermophoretic parameter N_t on nanoparticles. It is found that ϕ increases by increasing N_t. This increase in ϕ is due to the thermophoretic effects because increasingly thermophoretic effect generates the larger mass flux due to temperature gradient. Fig. 2.8 is plotted to perceive the effects of Le on nanoparticle concentration. It is observed that the concentration profile decreases and concentration boundary layer thins as Le increases. It is quite obvious because Le inversely proportional to mass diffusive coefficient.

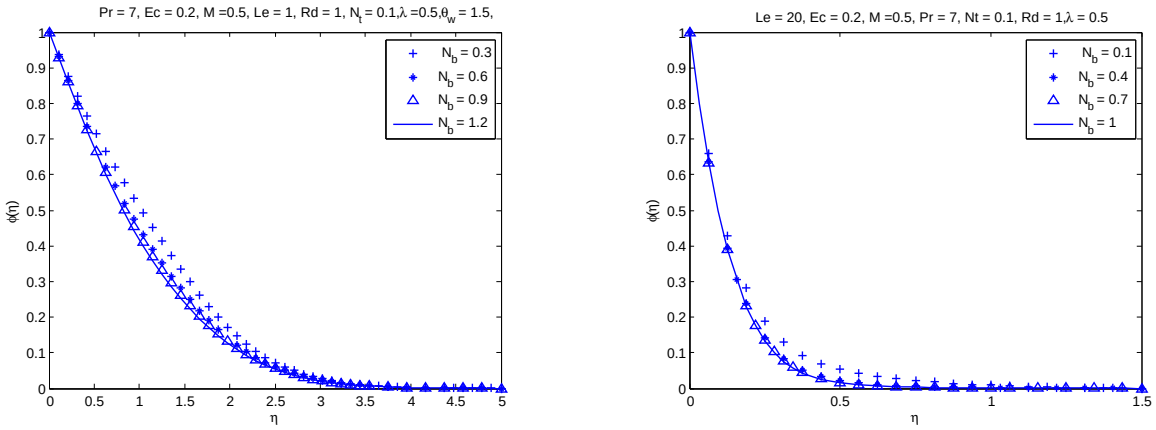

Figure 2.6: Influence of N_b on ϕ. (left CWT, right PST)

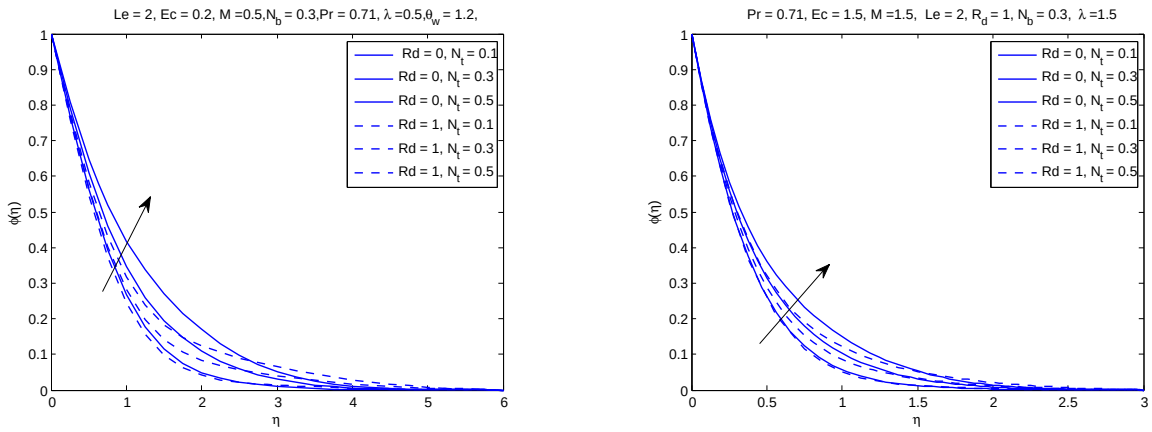

Figure 2.7: Influence of N_t on ϕ. (left CWT, right PST)

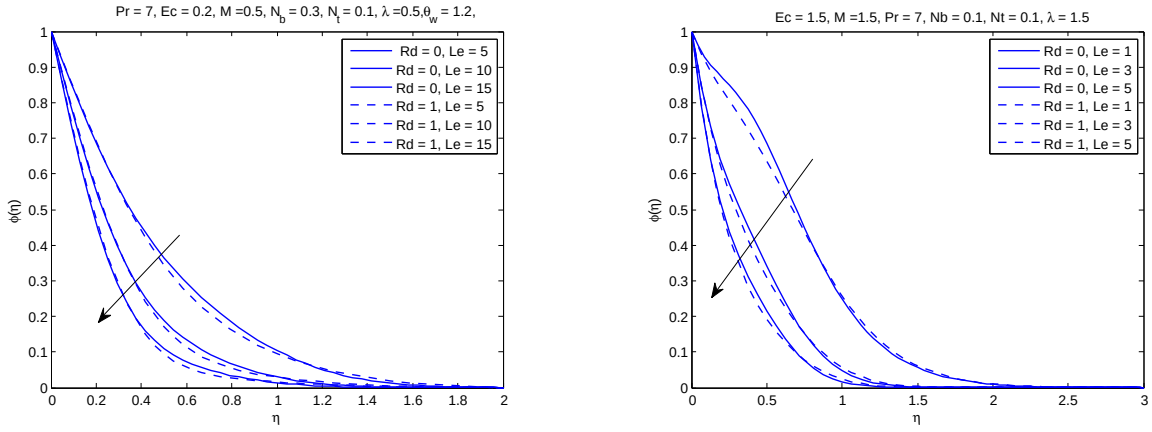

Figure 2.8: Influence of L_e on ϕ. (left CWT, right PST)

Chapter 3

Numerical Solution of Stagnation-Point Flow of Nanofluid Using Convective and Newtonian Heating Boundary Conditions

Chapter 3 is organized as follows.

Section 3.1 gives introduction. Section 3.2 and 3.3 contains a discussion on the derivation of the mathematical formulation of the problem. In section 3.4 we discuss the numerical results with the help of graphs and tables.

3.1 Introduction

This chapter is an extension of the work by Mustafa et al [7] described in chapter 2. This works explain the MHD stagnation-point flow and heat

transfer of nanofluid over a stretching sheet with convective and Newtonian heating boundary conditions. The problem with convective boundary condition have been solved by Mushtaq et al [8]. Strictly different application of Rosseland approximation for thermal radiation is made. The resulting partial differential equations have been solved numerically by shooting method with fifth order Runge-Kutta integration technique. The solutions have been verified with the built-in solver bvp4c of MATLAB. Graphs are portrayed for the effects of various parameters on the flow fields.

3.2 Mathematical Formulation

We consider the same governing equations of section 2.2 as given in chapter 2.

$$\frac{\partial u}{\partial x} + \frac{\partial v}{\partial y} = 0, \tag{3.2.1}$$

$$u\frac{\partial u}{\partial x} + v\frac{\partial v}{\partial y} = u_\infty \frac{du_\infty}{dx} + \nu_f \frac{\partial^2 u}{\partial y^2} - \frac{\sigma_e H_o^2}{\rho_f}(u - u_\infty), \tag{3.2.2}$$

where $x-$ and $y-$ are taken along and normal to the stretching sheet respectively, ν_f is the kinematic viscosity of fluid, σ_e is the electrical conductivity, H_o is uniform magnetic field along $y-$axis, the velocity components u and v are selected along $x-$ and $y-$ directions respectively. The boundary conditions for the governed problem are

$$u = U_w(x) = ax, \quad v = 0, \quad at \quad y = 0, \tag{3.2.3}$$

$$u \longrightarrow U_\infty(x) = bx, \qquad as \quad y \longrightarrow \infty. \tag{3.2.4}$$

Using the following similarity transformation

$$\eta = \sqrt{\tfrac{a}{\nu_f}}y\ , \qquad u = ax\acute{f}(\eta), \qquad v = -\sqrt{\nu}_f a f(\eta).$$

Eq. (3.2.1) is uniformly satisfied and Eqs. (3.2.2) (3.2.3) and (3.2.4) take the forms

$$f''' + ff'' - f'^2 + \lambda^2 + M(\lambda - f') = 0. \tag{3.2.5}$$

$$f(0) = 0, \quad f'(0) = 1, \quad f'(\infty) \longrightarrow \lambda. \tag{3.2.6}$$

In above equations $\lambda = \frac{b}{a}$ denotes the ratio of the free stream velocity to the velocity of the sheet and $M = \frac{\sigma H_o}{\rho f^a}$ indicates a magnetic parameter.

3.3 Transport Equations

The boundary layer equations governing the conservations of energy and nanoparticles field are

$$\begin{aligned} u\frac{\partial T}{\partial x} + v\frac{\partial T}{\partial y} = \quad & \alpha\frac{\partial^2 T}{\partial y^2} + \frac{\nu_f}{C_f}(\frac{\partial u}{\partial y})^2 - \frac{1}{(\rho C)_f}(\frac{\partial q_r}{\partial y}) + \frac{\sigma_e H_0^2}{(\rho C)_f} \\ & (u_\infty - u)^2 + \tau[D_B\frac{\partial T}{\partial y}\frac{\partial C}{\partial y} + \frac{D_T}{T_\infty}(\frac{\partial T}{\partial y})^2], \end{aligned} \tag{3.3.1}$$

$$u\frac{\partial C}{\partial x} + \frac{v\partial C}{\partial y} = D_B\frac{\partial^2 C}{\partial y^2} + \frac{D_T}{T_\infty}\frac{\partial^2 T}{\partial y^2}, \tag{3.3.2}$$

where T and C are the temperature and nanoparticles concentration respectively, α denotes the thermal diffusivity, C_f indicate the specific heat of the fluid, D_B and D_T are the Brownian motion and thermophoretic diffusion coefficient respectively, ($\tau = \frac{(\rho C)_p}{(\rho C)_f}$) is the fraction of effective heat capacity of the nanoparticle material to the heat capacity of the fluid and q_r is the radiative heat flux. From Rosselands approximation the radiative heat flux is modeled as

$$q_r = -\frac{4\sigma^*}{3k^*}\frac{\partial T^4}{\partial y} = -\frac{16\sigma^*}{3k^*}T^3\frac{\partial T}{\partial y}, \tag{3.3.3}$$

where σ^* is the Stefan-Boltzman constant and k^* is the mean absorption coefficient. Eq. (3.3.1) can be expressed as

$$u\frac{\partial T}{\partial x}+v\frac{\partial T}{\partial y}= \quad \frac{\partial}{\partial y}[(\alpha+\frac{16\sigma^* T^3}{3\rho C_p k^*})\frac{\partial T}{\partial y}]+\frac{\nu_f}{C_p}(\frac{\partial u}{\partial y})^2+\frac{\sigma_e H_0^2}{(\rho C)_f}$$
$$(u_\infty-u)^2+\tau[D_B\frac{\partial T}{\partial y}\frac{\partial C}{\partial y}+\frac{D_T}{T_\infty}(\frac{\partial T}{\partial y})^2]. \qquad (3.3.4)$$

3.3.1 Heat Transfer Analysis via Convective Boundary Condition (CBC)

The boundary conditions for our case are

$$-k\frac{\partial T}{\partial y}=h(T_f-T), \quad C=C_w \qquad at \qquad y=0, \quad (3.3.5)$$
$$T\longrightarrow T_\infty, \qquad C\longrightarrow C_\infty \qquad as \quad y\longrightarrow\infty. \qquad (3.3.6)$$

We now define the non-dimensional $\theta_\eta=\frac{T-T_\infty}{T_f-T_\infty}$ with $T=T_\infty(1+(\theta_w-1)\theta)$ and $\theta_w=\frac{T_f}{T_\infty}$ (temperature parameter), and the non-dimensional concentration $\phi(\eta)=\frac{C-C_\infty}{C_w-C_\infty}$.The first term on the right hand side of Eq. (3.3.4) can be written as $\alpha\frac{\partial}{\partial y}[\frac{\partial T}{\partial y}(1+R_d(1+\theta_w-1)\theta)^3]$, where $R_d=\frac{16\sigma^* T_\infty^3}{3kk^*}$ denotes the radiation parameter for the CWT case, and R_d provides no thermal radiation effect. The last expression can be further reduced to

$$\frac{\alpha(T_f-T_\infty)}{Pr}[(1+R_d(1+(\theta_w-1)\theta)^3)\theta']',$$

where Pr $=\frac{\nu}{a}$ is the Prandtl number. Eqs. (3.3.2) and (3.3.4) take the following forms

$$\frac{1}{Pr}[(1+R_d(1+(\theta_w-1)\theta)^3)\theta']'+ \quad f\theta'+N_b\theta'\phi'+N_t\theta'^2+E_c^* f''^2$$
$$+ME_c^*(\lambda-f')^2=0, \qquad (3.3.7)$$

$$\phi''+L_e f\phi'+\frac{N_t}{N_b}\theta''=0. \qquad (3.3.8)$$

with boundary conditions

$$\theta'(0) = -B(1-\theta(0)), \quad 0.1 \leq B < \infty, \quad \phi(0) = 1, \tag{3.3.9}$$

$$\theta \longrightarrow 0, \qquad \phi \longrightarrow 0, \qquad as \qquad \eta \longrightarrow \infty. \tag{3.3.10}$$

Where $N_b = \frac{\tau D_B(C_w - C_\infty)}{\nu_f}$ and $N_t = \frac{\tau D_T(T_f - T_\infty)}{T_\infty \nu_f}$ are denoted by Brownian and thermophoretic constants respectively and $E_c^* = \frac{U_w^2}{C_p(T_w - T_\infty)}$ indicates the local Eckert number. The heat and mass fluxes are defined by the equations given below.

$$q_w = -k(\frac{\partial T}{\partial y})_{y=0} + (q_r)_w = -R_d[\frac{B+\theta'(0)}{B}]^3(\theta_w^3)(\theta'(0)), \tag{3.3.11}$$

$$j_w = -D_B(\frac{\partial C}{\partial y})_{y=0} = -D_B(C_w - C_\infty)\sqrt{\frac{a}{\nu}}\phi_0', \tag{3.3.12}$$

use local Nusselt number $Nu_x = \frac{xq_w}{k(T_f - T_\infty)}$ and local Sherwood number $Sh = \frac{xj-w}{D_B(c_w - c_\infty)}$ in above equations, one obtains $\frac{Nu_x}{\sqrt{Re_x}} = [1 + R_d(\frac{B+\theta'(0)}{B})^3\theta_w^3]\theta'(0) = Nu_r$, $\frac{Sh}{\sqrt{Re_x}} = -\phi(0) = Shr$.

3.3.2 Heat Transfer Analysis via Newtonian Heating (NH)

The relevant boundary conditions in this case are

$$-k\frac{\partial T}{\partial y} = h_s T, \quad C = C_w \qquad at \qquad y = 0, \tag{3.3.13}$$

$$T \longrightarrow T_\infty, \qquad C \longrightarrow C_\infty \qquad as \quad y \longrightarrow \infty. \tag{3.3.14}$$

For Newtonian heating the non-dimensional temperature is $\theta(\eta) = \frac{T - T_\infty}{T_\infty}$ with $T = T_\infty(1+\theta)$.

By using this transformation of θ. The Eq. (3.3.4) takes the following form

$$\frac{1}{Pr}[(1 + R_d(1+\theta)^3)\theta']' + \quad f\theta' + N_b\theta'\phi' + N_t\theta'^2 + E_c^* f''^2 + ME_c^*(\lambda - f')^2 = 0, \tag{3.3.15}$$

with boundary conditions

$$\theta'(0) = -B^*(1+\theta(0)), \quad 0.1 \leq B^* < \infty, \quad \phi(0) = 1, \quad (3.3.16)$$

$$\theta \longrightarrow 0, \qquad \phi \longrightarrow 0, \qquad as \qquad \eta \longrightarrow \infty. \qquad (3.3.17)$$

In above Equation
$B^* = h_s\sqrt{\frac{\nu_f}{a}}$,
$N_b = \frac{\tau D_B(C_w - C_\infty)}{\nu_f}$,
$N_t = \frac{\tau D_T}{\nu_f}$,
$E_c^* = \frac{U_w^2}{C_p(T_\infty)}$.
The reduced Nusselt number in this case is $\frac{Nu_x}{\sqrt{Re_x}} = B^*[1 + \frac{1}{\theta(0)}](1 + R_d(1 + \theta(0))^3) = Nu_r$.

3.4 Numerical Results and Discussion

The numerical solution of governing differential systems for different values of thermophoretic parameter N_t, Brownian parameter N_b and thermal radiation parameter Rd is obtained using shooting method with fifth order Runge-Kutta integration technique. After reducing the relevant equations to the first order systems, suitable values of missing slopes $f''(0)$, $\theta'(0)$ and $\phi'(0)$ are chosen and then successive iteration are performed using Newton's method until the boundary condition at sufficiently large value of η is satisfied. To examine the physical effects of the embedded parameters, we have plotted Figs. 3.1-3.4 and prepared table.

3.4.1 Heat and Mass Transfer Rates

In this subsection we discuss the behavior and numerical results of $\theta'(0)$ and $\phi'(0)$ for various parametric values. Table provide such values in our case. It

is seen that heat and mass flux from the sheet decreases as thermal radiation strengthens. For fixed value of thermophoretic parameter there is decrease in $|\theta'(0)|$ with an increase in N_b. This decrease is in fact due to effective movement of nanoparticles from the stretching wall to the quiescent fluid. It is observed that the reduced Sherwood number considerably increases when N_b is increased. The impact of N_b on the reduced Nusselt number and Sherwood number is similar with and without R_d influence. For a fixed N_b there is decrease in the magnitude of reduced Nusselt number with an increase in N_t or equivalently the mass flux due to temperature gradient. However mass transfer rate at the sheet is found to increase upon increasing thermophoretic constant with and without R_d effects.

Table 1. Value of dimensionless heat transfer rate $-\theta'(0)$ and dimensionless mass transfer rate $-\phi'(0)$ for different values of the Nb, Nt and Rd when $\lambda = 0.5$, M=0.5, Pr=7, Le=1, Ec=0.2, B=0.2 in the CWT case.

N_b	N_t	R_d	$-\theta'(0)$ shooting method	$-\theta'(0)$ bvp4c	$-\phi'(0)$ shooting method	$-\phi'(0)$ bvp4c
0.1	0.1	0	0.15457	0.15457	0.63968	0.63967
		1	0.15198	0.15198	0.63764	0.63763
0.2		0	0.14786	0.14786	0.67761	0.67761
		1	0.14763	0.14763	0.67265	0.67265
0.3		0	0.13963	0.13963	0.69149	0.69149
		1	0.14284	0.14284	0.68460	0.68460
0.4		0	0.12950	0.12950	0.69955	0.69955
		1	0.13760	0.13760	0.69079	0.69079
0.1	0.1	0	0.15457	0.15457	0.63968	0.63967
		1	0.15198	0.15198	0.63764	0.63763
	0.2	0	0.15351	0.15351	0.58798	0.58797
		1	0.15125	0.15125	0.58159	0.58159
	0.3	0	0.15236	0.15236	0.54269	0.54268
		1	0.15049	0.15049	0.52922	0.52921
	0.4	0	0.15111	0.15111	0.50459	0.50458
		1	0.14968	0.14968	0.48074	0.48074

3.4.2 Velocity Profile

The dimensionless velocity boundary profile is same as we have discussed in chapter 2. (Cf. subsection 2.4.2).

3.4.3 Temperature Profiles

We have already discussed the effects of N_b, N_t, and R_d on temperature θ in chapter 2. So we will discuss here only our extended work. Fig 3.1 illustrates that the temperature increases with an increase in the Biot number. It is indicated that the thermal resistance of sheet decreases and convective heat transfer to the fluid increases when Biot number effect intensifies. Fig. 3.2 shows that by increasing Newtonian heat parameter B^* temperature θ also increases. Fig. 3.3 and 3.4 depicts the influence of Pr on temperature profile. It is seen that temperature decreases and thermal boundary layer thins as Pr increases in both CBC and NH cases. This decrease is related with the steeper temperature profile and consequently, large rate of heat transfer at the bounding surface.

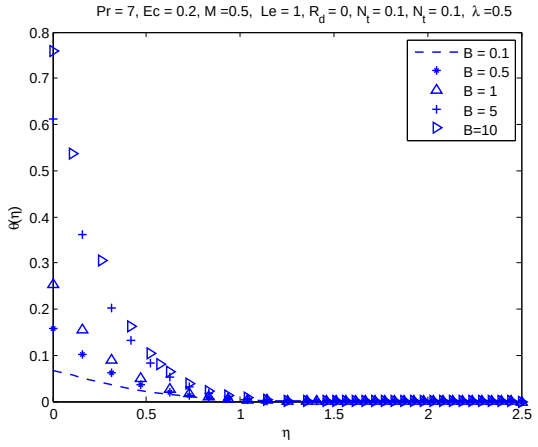

Figure 3.1: Influence of B on θ (for CBC case).

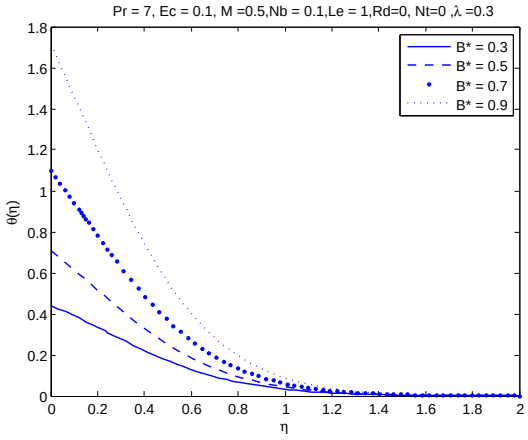

Figure 3.2: Influence of B^* on θ (for NH case).

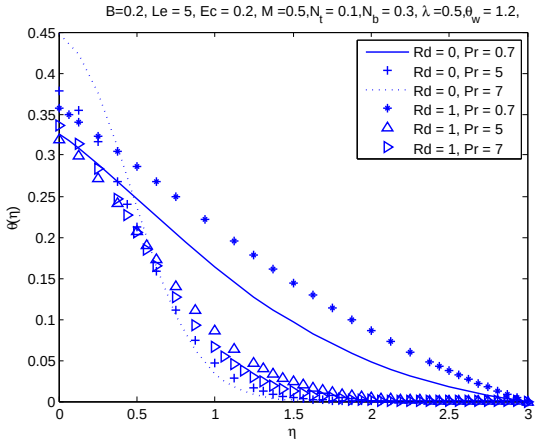

Figure 3.3: Influence of P_r on θ (for CBC case).

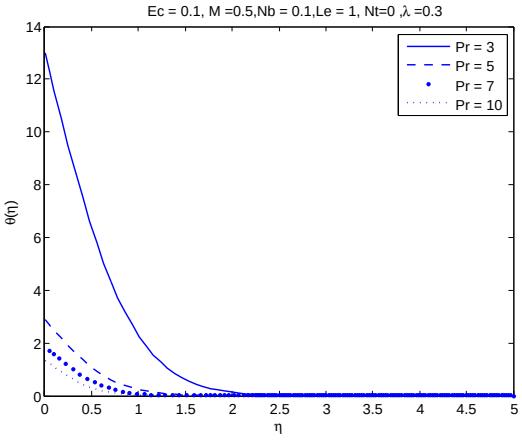

Figure 3.4: Influence of Pr on θ (for NH case).

3.4.4 Nanoparticles Concentration Profiles

Fig. 3.5 is displayed to observe the effects of Brownian motion parameter N_b on the nanoparticles concentration ϕ. We observe that by increasing Brownian motion parameter ϕ remains almost constant. So, rate of mass transfer constant for Nb. Fig. 3.6 indicates that concentration and the concentration boundary layer thickness increase when thermophoretic effect intensifies. This is not surprising since increasing thermophoretic effect generates the larger mass flux due to temperature gradient which in turn raises the nanoparticles volume fraction ϕ. The concentration field is driven by the temperature gradient and since temperature is an increasing function of Rd, thus one would expect an increase in the concentration ϕ with an increase in Rd. Fig. 3.7 shows that nanoparticles concentration decreases and concentration boundary layer thins as Lewis number increase. We can also interpret that rate of heat and mass transfer decrease with increase in N_t.

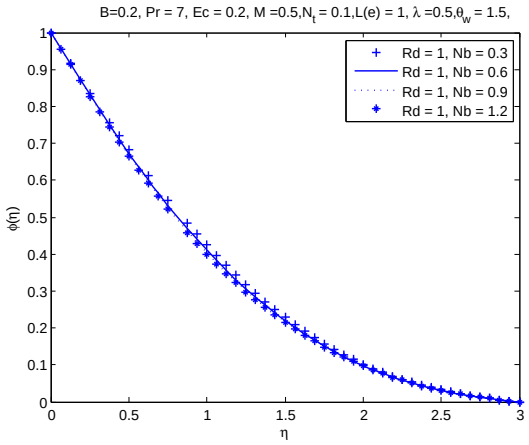

Figure 3.5: Influence of N_b on ϕ (for CBC case).

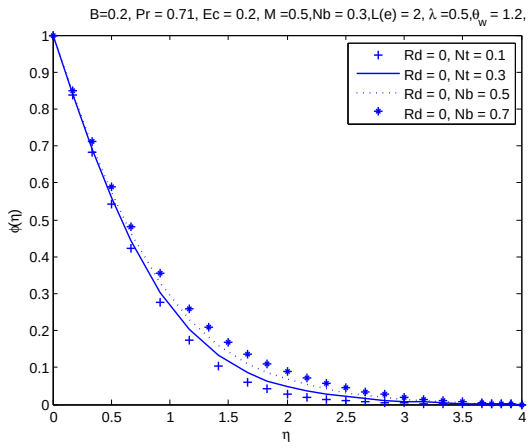

Figure 3.6: Influence of N_t on ϕ (for CBC case).

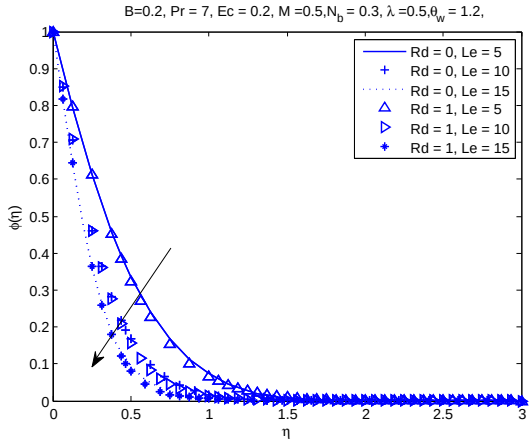

Figure 3.7: Influence of L_e on ϕ (for CBC case).

Chapter 4

Viscous Compressible Boundary Layer Flow on a Moving Flat Plate in a Parallel Free Stream

Chapter 4 is divided into the following sections.

Section 4.1 is the introduction of problem. Section 4.2 includes a discussion on the derivation of the mathematical formulation of the boundary layer flow with variable fluid properties on a moving flat plate in a parallel free stream. In section 4.3 we discuss two special cases, constant fluid properties and variable fluid properties. In section 4.4 we discuss the numerical results with the help of graphs and tables.

4.1 Introduction

This chapter deals with the numerical study of steady boundary layer flows of compressible fluids. This chapter is a review work of Bachok et al [9]. In this chapter two special cases are considered: constant fluid properties and variable fluid properties. The resulting differential equations have been solved by shooting method and bvp4c. Numerical outcomes for the flow and the thermal fields for both cases are obtained for various parametric values of free stream and the prandtl number.

4.2 Problem Formulation

The steady two dimensional compressible boundary layer equation are given as Andersson and Aarseth [10].

$$\frac{\partial}{\partial x}(\rho u) + \frac{\partial}{\partial y}(\rho v) = 0, \tag{4.2.1}$$

$$\rho(u\frac{\partial u}{\partial x} + v\frac{\partial u}{\partial y}) = \frac{\partial}{\partial y}(\mu\frac{\partial u}{\partial y}), \tag{4.2.2}$$

$$\rho c_p(u\frac{\partial T}{\partial x} + v\frac{\partial T}{\partial y}) = \frac{\partial}{\partial y}(k\frac{\partial T}{\partial y}). \tag{4.2.3}$$

The relevant boundary conditions are

$$u = U_w, \qquad v = 0, \qquad T = T_w, \qquad at \qquad y = 0, \tag{4.2.4}$$

$$u \to U_o, \qquad T \to T_o, \qquad as \qquad y \to \infty. \tag{4.2.5}$$

In above equation

ρ= fluid density

u, v= velocities in x and y directions

μ = dynamic viscosity

k= thermal conductivity

C_p = specific heat.

We introduce now the similarity transformation and the dependent variable f and θ are defined as, see Andersson and Aarseth [10],

$$\begin{aligned} \eta &= (\frac{U}{av_o x})^{1/2} \int (\frac{\rho}{\rho_o}) dy, && (4.2.6) \\ \psi(x,y) &= \rho_o (a\nu_o x U)^(1/2) f(\eta), && (4.2.7) \\ \theta(\eta) &= \frac{T - T_o}{T_w - T}. && (4.2.8) \end{aligned}$$

Where $U = U_w + U_o$, is a dimensionless constant and ψ is the stream function, which is described as

$$\rho u = \frac{\partial \psi}{\partial y}, \quad \rho v = -\frac{\partial \psi}{\partial x} \tag{4.2.9}$$

ρ_o, μ_o, k_o, C_{po} and ν_o denotes the values of fluid properties of the ambient fluid at ambient temperature T_o. Now we use Eqs. (4.2.6), (4.2.7) and (4.2.9) to find u and v.

$$\begin{aligned} \rho u &= \rho_o (a\nu_o x U)^{1/2} f'(\eta) (\frac{U}{a\nu_o x})^{1/2} \frac{d}{dy} \int \frac{\rho}{\rho_o} dy \\ , \rho u &= \rho_o (a\nu_o x U)^{1/2} f'(\eta) (\frac{U}{a\nu_o x})^{1/2} \frac{d}{dy} (\frac{\rho}{\rho_o}), \\ \rho u &= \rho U f'(\eta), && (4.2.10) \end{aligned}$$

$$\begin{aligned} \rho v = [\frac{\rho_o}{2} (\frac{1}{a\nu_o x U})^{1/2} (a\nu_o U) f(\eta) + & \quad \rho_o (a\nu_o x U)^{1/2} f'(\eta) \frac{1}{2} (\frac{a\nu_o x}{U})^{1/2} \\ & (\frac{-U}{a\nu_o x^2}) \int \frac{\rho}{\rho_o} dy], \end{aligned}$$

$$\rho v = -\frac{\rho_o}{2} (\frac{a\nu_o U}{x})^{1/2} f(\eta) + \frac{U}{x} \frac{\rho_o}{2} f'(\eta) \int \frac{\rho}{\rho_o} dy. \tag{4.2.11}$$

Now we convert the Eqs. (4.2.2) and (4.2.3) into ODEs

$$\begin{aligned}
\frac{\partial u}{\partial x} &= Uf''(\eta)\frac{1}{2}(\frac{a\nu_o x}{U})^{1/2}(-\frac{U}{a\nu_o x^2})\int\frac{\rho}{\rho_o}dy,\\
\rho u\frac{\partial u}{\partial x} &= -\frac{\rho U^2}{2x}f'(\eta)f''(\eta)(\frac{U}{a\nu_o x})^{\frac{1}{2}}\int\frac{\rho}{\rho_o}dy, \qquad (4.2.12)\\
\rho v\frac{\partial u}{\partial y} &= [-\frac{\rho_o}{2}(\frac{a\nu_o U}{x})^{1/2}f(\eta)+\frac{U}{x}\frac{\rho_o}{2}f'(\eta)\int\frac{\rho}{\rho_o}dy]Uf''(\eta)(\frac{U}{a\nu_o x})^{\frac{1}{2}}\frac{\rho}{\rho_o},\\
\rho v\frac{\partial u}{\partial y} &= -\frac{\rho U^2}{2x}f(\eta)f''(\eta)+\frac{\rho U^2}{2x}f'(\eta)f''(\eta)(\frac{U}{a\nu_o x})^{\frac{1}{2}}\int\frac{\rho}{\rho_o}dy, \qquad (4.2.13)\\
\frac{\partial}{\partial y}(u\frac{\partial u}{\partial y}) &= \frac{\partial}{\partial y}(\mu Uf''(\eta)(\frac{U}{a\nu_o x})^{\frac{1}{2}}\frac{\rho}{\rho_o}). \qquad (4.2.14)
\end{aligned}$$

Use this in Eq. (4.2.14)

$$\begin{aligned}
\frac{\partial}{\partial y}(u\frac{\partial u}{\partial y}) &= \frac{\partial}{\partial\eta}(\mu f''(\eta))(U(\frac{U}{a\nu_o x})^{\frac{1}{2}}\frac{\rho}{\rho_o})(\frac{U}{a\nu_o x})^{\frac{1}{2}}(\frac{\rho}{\rho_o}),\\
\frac{\partial}{\partial y}(u\frac{\partial u}{\partial y}) &= (\mu f''(\eta))'\frac{U^2}{a\nu_0 x}\frac{\rho^2}{\rho_o^2}. \qquad (4.2.15)
\end{aligned}$$

Put Eqs. (4.2.12), (4.2.13) and (4.2.15) in Eq. (4.2.2) we get

$$\begin{aligned}
-\frac{\rho U^2}{2x}f'(\eta)f''(\eta)(\frac{U}{a\nu_o x})^{\frac{1}{2}}\int\frac{\rho}{\rho_o}dy-\frac{\rho U^2}{2x}f(\eta)f''(\eta)+\quad &\frac{\rho U^2}{2x}f'(\eta)f''(\eta)\\
(\frac{U}{a\nu_o x})^{\frac{1}{2}}\int\frac{\rho}{\rho_o}dy=(\mu f''(\eta))'\quad &\frac{U^2}{a\nu_o x}\frac{\rho^2}{\rho_o^2},\\
-\frac{\rho}{2}\frac{U^2}{x}f(\eta)f''(\eta)=(\mu f''(\eta))'\frac{U^2}{a\nu_o x}\frac{\rho^2}{\rho_o^2},&\\
\frac{2}{a}(\frac{\rho}{\rho_o}\frac{\mu}{\mu_o}f''(\eta))'+f(\eta)f''(\eta)=0. \qquad (4.2.16)&
\end{aligned}$$

Now we convert Eq. (4.2.3) into ODEs From Eq. (4.2.8)

$$T=(T_w-T_o)\theta(\eta)+T_o, \qquad (4.2.17)$$

$$\begin{aligned}
C_p(\rho u)\frac{\partial T}{\partial x} &= C_p(\rho Uf'(\eta))\theta'(\eta)(\frac{T_w-T_o}{2})(\frac{a\nu_o x}{U})^{\frac{1}{2}}(-\frac{U}{a\nu_o x^2})\int\frac{\rho}{\rho_o}dy,\\
C_p(\rho u)\frac{\partial T}{\partial x} &= -C_p(\rho Uf'(\eta))\theta'(\eta)(\frac{T_w-T_o}{2})(\frac{U}{a\nu_o x})^{\frac{1}{2}}\frac{1}{x}\int\frac{\rho}{\rho_o}dy,\\
C_p(\rho u)\frac{\partial T}{\partial x} &= -C_p\frac{\rho U}{2x}f'(\eta)\theta'(\eta)(T_w-T_o)(\frac{U}{a\nu_o x})^{\frac{1}{2}}\int\frac{\rho}{\rho_o}dy, \qquad (4.2.18)\\
C_p(\rho v)\frac{\partial T}{\partial y} &= C_p[-\frac{\rho_o}{2}(\frac{a\nu_o U}{x})^{1/2}f(\eta)+\frac{U}{x}\frac{\rho_o}{2}f'(\eta)\int\frac{\rho}{\rho_o}dy](T_w-T_o)\theta'(\eta)(\frac{U}{a\nu_o x})^{\frac{1}{2}}\frac{\rho}{\rho_o},
\end{aligned}$$

$$C_p(\rho v)\frac{\partial T}{\partial y} = -C_p\frac{\rho U}{2x} \qquad (T_w - T_o)f(\eta)\theta'(\eta) + C_p\frac{\rho U}{2x}(T_w - T_o)$$
$$f'(\eta)\theta'(\eta)(\frac{U}{a\nu_o x})^{\frac{1}{2}}\int\frac{\rho}{\rho_o}dy, \tag{4.2.19}$$

$$\begin{aligned}
\frac{\partial}{\partial y}(k\frac{\partial T}{\partial y}) &= \frac{\partial}{\partial y}[k\theta'(\eta)(T_w - T_o)(\frac{U}{a\nu_o x})^{\frac{1}{2}}\frac{\rho}{\rho_o}], \\
\frac{\partial}{\partial y}(k\frac{\partial T}{\partial y}) &= \frac{\partial}{\partial \eta}(k\theta'(\eta))(T_w - T_o)(\frac{U}{a\nu_o x})^{\frac{1}{2}}\frac{\rho}{\rho_o}(\frac{U}{a\nu_o x})^{\frac{1}{2}}\frac{\rho}{\rho_o}, \\
\frac{\partial}{\partial y}(k\frac{\partial T}{\partial y}) &= (k\theta'(\eta))'(T_w - T_o)\frac{U}{ax(\rho_o\nu_o)}\frac{\rho_2}{\rho_o^2}.
\end{aligned} \tag{4.2.20}$$

Put Eqs. (4.2.18),(4.2.19) and (4.2.20) in Eq. (4.2.3)

$$-C_p\frac{\rho U}{2x}f'(\eta)\theta'(\eta)(T_w - T_o) \qquad (\frac{U}{a\nu_o x})^{\frac{1}{2}}\int\frac{\rho}{\rho_o}dy - C_p\frac{\rho U}{2x}(T_w - T_o)f(\eta)\theta'(\eta)$$
$$+C_p\frac{\rho U}{2x}(T_w - T_o)f'(\eta)\theta'(\eta) \qquad (\frac{U}{a\nu_o x})^{\frac{1}{2}}\int\frac{\rho}{\rho_o}dy =$$
$$(k\theta'(\eta))'(T_w - T_o)\frac{U}{ax(\rho_o\nu_o)}\frac{\rho_2}{\rho_o^2}, \tag{4.2.21}$$

$$\begin{aligned}
\frac{1}{a\mu_o}(k\frac{\rho}{\rho_o}\theta'(\eta))' + \frac{C_p}{2}f(\eta)\theta'(\eta) &= 0, \\
\frac{1}{a\mu_o}(k\frac{\rho}{\rho_o}\theta'(\eta))'\frac{1}{2}\frac{C_p}{C_{p_o}}\frac{C_{p_o}\mu_o}{k_o}\frac{k_0}{\mu_o}f(\eta)\theta'(\eta) &= 0, \\
(\frac{k}{k_o}\frac{\rho}{\rho_o}\theta'(\eta))' + \frac{a}{2}\frac{C_p}{C_{p_o}}P_{r_o} + f(\eta)\theta'(\eta) &= 0.
\end{aligned} \tag{4.2.22}$$

Where Pr_o denotes the prandtl number of the ambient fluid and prime represent differentiation with respect to η. Now we convert boundary condition into ODEs From Eq. (4.2.5) we know that

$$u = U_w,$$

and from Eq. (4.2.10)

$$u = Uf'(\eta),$$

compare both values when $\eta = 0$ and $y = 0$

given that

$$\begin{aligned} U &= U_w + U_o, \qquad (4.2.23) \\ U - U_o &= U f'(0), \\ 1 - \frac{U_o}{U} &= f'(0), \\ 1 - \epsilon &= f'(0). \qquad (4.2.24) \end{aligned}$$

From Eq. (4.2.5)

$$v = 0 \qquad \text{when} \qquad y = 0.$$

From Eq. (4.2.11)

$$\frac{1}{\rho}[-\frac{\rho_o}{2}(\frac{a\nu_o U}{x})^{1/2} f(\eta) + \frac{U}{x}\frac{\rho_o}{2} f'(\eta) \int \frac{\rho}{\rho_o} dy],$$

by comparing both values of v we get

$$f(0) = 0. \qquad (4.2.25)$$

again from Eq. (4.2.5)

$$T = T_w, \qquad \text{when} \qquad y = 0$$

from Eq. (4.2.17) when $\eta = 0$

$$T = (T_w - T_o)\theta(\eta) + T_o,$$

after comparing both values of T we get,

$$\theta(0) = 1. \qquad (4.2.26)$$

From Eq. (4.2.6)

$$u \to U_o \qquad \text{when} \qquad y \to \infty$$

and from Eq. (4.2.10) when $\eta \to \infty$ then

$$u = Uf'(\infty),$$

by comparing both values we get

$$\begin{aligned} \frac{U_o}{U} &= f'(\infty), \\ \epsilon &= f'(\infty). \end{aligned} \tag{4.2.27}$$

Again from Eq. (4.2.6)

$$T \to T_o \qquad when \qquad y \to \infty$$

and from Eq. (4.2.17) when $\eta = 0$

$$T = (T_w - T_o)\theta(\eta) + T_o,$$

by comparing above values we get

$$\theta(\infty) = 0. \tag{4.2.28}$$

Eq. (4.2.23) to Eq. (4.2.27) are new boundary conditions subjected to Eqs. (4.2.4) and (4.2.5)

$$f(0) = 0, \qquad f'(0) = 1 - \epsilon, \qquad \theta(0) = 1 \qquad \eta = 0, \tag{4.2.29}$$

$$f'(\eta) = \epsilon, \qquad \theta(\eta) = 0, \qquad as \qquad \eta \to \infty. \tag{4.2.30}$$

Where ϵ is free stream parameter and is defined as

$$\epsilon = \frac{U_o}{U} = \frac{U_o}{U_o + U_w}. \tag{4.2.31}$$

In above equation $\epsilon = \frac{1}{2}$, $\epsilon = 1$ and $\epsilon = 0$ corresponds to the different flow regimes. For $\epsilon = \frac{1}{2}$ it corresponds to a free stream velocity and $\epsilon = 1$ shows

the behavior of Blasius flow and $\epsilon = 0$ is for Sakiadis flow. The important quantities of interest are shear stress and heat flux q_w which are given as

$$\tau_w = \mu_w(\frac{U^3}{a\nu_o x})^{\frac{1}{2}} f''(0), \tag{4.2.32}$$

$$q_w = \mu_w C_{p_o} P_{r_o}^{-1} \Delta T(\frac{U}{a\nu_o x})^{\frac{1}{2}}[-\theta'(0)]. \tag{4.2.33}$$

4.3 Special Cases

4.3.1 Constant Fluid Properties (Case A)

This case corresponds to the Blasius [1] flow variable.

$$\eta = (\frac{U}{a\nu_0 x})^{\frac{1}{2}} y. \tag{4.3.1}$$

In this case $\frac{\rho}{\rho_o} = 1$, $\frac{\mu}{\mu_o} = 1$, $\frac{k}{k_o} = 1$ and $\frac{C_p}{C_{p_o}} = 1$ so Eqs. (4.2.16) and (4.2.22) reduces to

$$\frac{2}{a} f'''(\eta) + f(\eta) f''(\eta) = 0, \tag{4.3.2}$$

$$\theta''(\eta) + \frac{a}{2} P_{r_o} f(\eta)\theta(\eta) = 0. \tag{4.3.3}$$

4.3.2 Variable Viscosity (Case B)

In this case the Eq. (4.2.16) becomes

$$\frac{2}{a}(\frac{\mu}{\mu_o} f''(\eta)) + f(\eta) f''(\eta) = 0. \tag{4.3.4}$$

Following the form of the variable viscosity $\mu(T)$ proposed by Lai and Kulacki, and used Andersson and Aarseth [10], we take $\mu(T)$ as

$$\mu(T) = \frac{\mu_{ref}}{1 + \gamma(T - T_{ref})}, \tag{4.3.5}$$

in which γ is a fluid property. Generally, Viscosity depends on temperature and it decrease with increasing temperature for liquids. For gases viscosity increases by increasing temperature.

$$\mu(T) = \frac{\mu_o}{1 - \frac{T - T_o}{(T_w - T_o)\theta_{ref}}} = \frac{\mu_o}{1 - \frac{\theta(\eta)}{\theta_{ref}}}. \tag{4.3.6}$$

4.4 Results and Discussions

The nonlinear ordinary differential Equations (ODEs) given in (4.3.2) or (4.3.4), depending on the actual case considered, along Eq. (4.3.3) subject to the boundary conditions in Eq. (4.2.29) and Eq. (4.2.30) were solved numerically using a shooting method and bvp4c. The author of paper [9] have solved this problem with finite difference scheme or Keller-Box method. We prove the same results by using shooting method and MATLAB built-in solver bvp4c.

We just compare our results with the results reported by [9], [10]. We come to conclude that the values of $f''(0)$ and $\theta'(0)$ obtained in this study are in very good agreement with the results reported by [9], [10].

In Table 1 and Table 2 the results for $f''(0)$ and $\theta'(0)$ are taken from the paper by Bachok et al [9].

Table 1 (Norfifah and Anuar [9])

Value of reduced skin friction coefficient $f''(0)$ and reduced heat flux $\theta'(0)$.

ϵ	Pr	a	Andersson [10]		Norfifah et al. [9]	
			f''	θ'	f''	θ'
0	0.7	1	0.4437483	0.3492365	0.4437	0.3492
0	1	1	-	-	0.4437	0.4437
0	10	1	-	-	0.4437	1.6803

Table 2 (Norfifah and Anuar [9])

Values of reduced skin friction coefficient $f''(0)$ and reduced heat flux $\theta'(0)$.

ϵ	Pr	a	Andersson [10]		Norfifah et al. [9]	
0	10	1	-f"(0)	$-\theta'(0)$	$-f''(0)$	$-\theta'(0)$
Case A			0.443748	1.680293	0.4437	1.6803
Case B			1.300553	1.529151	1.3006	1.5292
0	1	1				
Case A			-	-	0.4437	0.4437
Case B			-	-	1.0381	0.3181

Table 3 (Current Results)

Value of reduced skin friction coefficient $f''(0)$ and reduced heat flux $\theta'(0)$.

ϵ	Pr	a	bvp4c		Shooting Method	
			f''	θ'	f''	θ'
0	0.7	1	0.4437	0.3492	0.4437	0.3492
0	1	1	0.4437	0.4437	0.4437	0.4437
0	10	1	0.4437	1.6803	0.4437	1.6803

Table 4 (Current Results)

Values of reduced skin friction coefficient $f''(0)$ and reduced heat flux $\theta'(0)$.

ϵ	Pr	a	bvp4c		Shooting Method	
0	10	1	$-f''(0)$	$-\theta'(0)$	$-f''(0)$	$-\theta'(0)$
Case A			0.4437	1.6803	0.4437	1.6803
Case B			1.3006	1.5292	1.3006	1.5292
0	1	1				
Case A			1.3006	1.5292	0.4437	0.4437
Case B			1.3006	1.5292	1.0381	0.3181

In Fig. 4.1 we can see that the velocity profile f' have been reduced near the surface in Case B. The viscosity is reduce due to heating of fluid by surface. In Fig. 4.2 we show the effect of Pr on temperature in Case A and B. We can see that the temperature decrease.

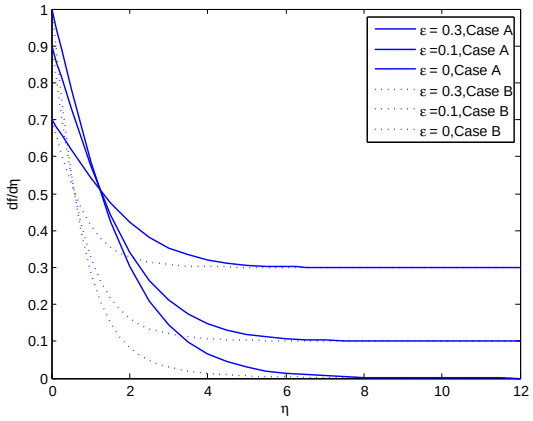

Figure 4.1: Velocity profiles $f'(\eta)$.

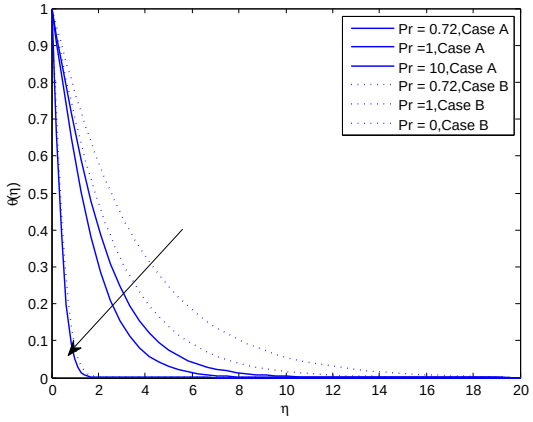

Figure 4.2: Temperature profiles $\theta(\eta)$.

Chapter 5

Conclusions and Outlook

This chapter contains an overview of the study as well as suggestions for the future research. The research considered in this dissertation is focused on the numerical solution for incompressible nanofluid and compressible regular fluid.

Chapter 1 include basic definitions. In chapter 2, the governing equations for boundary layer flow of nanofluid is presented first. Then we convert PDEs into ODEs with the help of similarity transformation. The resulting non-linear ODEs have been solved for the numerical solution by fifth order Runge-Kutta method using a shooting technique and verify the results with bvp4c. In this chapter we discussed the velocity, temperature and concentration profiles for different values of parameters.

Chapter 3 is an extension of the work described in chapter 2. In this chapter we solve the governing equations of chapter 2 with convective boundary condition. The dimensionless coupled equations have been solved by fifth order Runge-Kutta method using shooting technique. We discuss here only Biot number effect on the temperature profile because all other effect have been discussed in chapter 2.

The temperature θ and thermal boundary layer thickness increase with an increase in the Biot number. Since as B increases, the thermal resistance of the sheet decreases and convective heat transfer to the fluid of the sheet increases.

Chapter 4 is the review work. In chapter 4, the governing equations for the compressible flow are given. The governing partial differential equations are transformed using similarity transformation to a more convenient form for numerical computation. The transformed nonlinear ordinary differential equations were solved numerically using the Keller-Box method in the work of work Bachok et al [9]. But we used shooting method and bvp4c. Numerical results for the skin friction coefficient and the local Nusselt number as well as the temperature profiles are illustrated in two tables and some graphs for various parameters. Two special cases, namely constant fluid properties and variable fluid viscosity were considered. The velocity f' reduced near the moving surface for case B as compared to case A.

The work on incompressible flows can be further extended for exponential stretching sheet. We have only considered the steady flow cases but unsteady flow can be done in future. The same is true for compressible boundary layer flow where one can consider unsteady case. Moreover, the Keller-Box method can be developed to solve the incompressible and compressible flows. In future one can also use other numerical open source software chebfun.

Bibliography

[1] H. Blasius, Grenzschichten in Flussigkeiten mit Kleiner Reibung, Z. Angew. Math. Phys. 56 (1908) 1-37.

[2] B. C. Sakiadis, Boundary-layer behaviour on continuous solid surfaces. I. Boundary-layer equations for two-dimensional and axisymmetric flow, AIChE J 7 (1961) 26-28.

[3] L. J. Crane, Flow past a stretching plate, Zeitschrift Fur Angewandte Mathematik Und Physik 7 (1961) 21-28.

[4] S. U. S. Choi, Enhancing thermal conductivity of fluids with nanoparticles. ASME Int Mech Eng 1995;66:99105.

[5] R. Cortel, About termal radiation effects on the magneto-hydrodynamic flow near the stagnation point of a stretching sheet.

[6] A. Alsaedi, M. Awais and T. Hayat, Effects of heat generation/absorption on stagnation point flow of nanofluid over a surface with convective boundary conditions, CNSNS 17 (2012) 42104223.

[7] M. Mustafa, M. Asif Farooq, T. Hayat and A. Alsaedi, Stagnation Point flow of nanofluid through different utilization of thermal radiation effect. [In press]

[8] A. Mushtaq, M. Mustafa, T. Hayat, A. Alsaedi, Nonlinear radiative heat transfer in the flow of nanofluid due to solar energy: A numerical study. [In press]

[9] N. Bachok, A. Ishak, R. Nazar and I. pop, Boundary layer flow with variable fluid properties on a moving flat plate in a parallel free stream, ZAMM.

[10] H. I. Andersson, J. B. Aarseth (2007) Sakiadis flow with variable fluid properties revisited. Int J Eng Sci 45:554-561.

[11] L. F. Shampine, J. Kierzenka, M. W. Reichelt (2003) solving boundary value problems for ordinary differential equations in MATLAB with bvp4c Tutorial Notes. Available at http://www.mathsworks.com.

Appendix

Subroutines for the Shooting Method

Subroutines of shooting method used in chapter 2, 3 and 4.

Subroutine of Newton-Raphson method

```
function root = newtonRaphson2(func,x,tol)
if nargin == 2; tol = 1.0e4*eps; end
if size(x,1) == 1; x = x'; end
for i = 1:30
    [jac,f0] = jacobian(func,x);
if sqrt(dot(f0,f0)/length(x)) < tol
root = x; return
end
dx = jac/(-f0)
x = x + dx;
if sqrt(dot(dx,dx)/length(x)) < tol*max(abs(x),1.0)
root = x; return
end
disp(i)
end
error('Too many iterations')
```

Jacobian is calculated here.

```
function [jac,f0] = jacobian(func,x)
h = 1.0e-4;
n = length(x);
```

```
jac = zeros(n);
f0 = feval(func,x);
for i =1:n
    temp = x(i);
x(i) = temp + h;
f1 = feval(func,x);
x(i) = temp;
jac(:,i) = (f1 - f0)/h;
end.
```

Here is a Subroutine of Runge-Kutta method.

```
function [xSol,ySol] = runKut5(dEqs,x,y,xStop,h,eTol)
if size(y,1) > 1 ; y = y'; end
if nargin < 6; eTol = 1.0e-6; end
n = length(y);
A = [0 1/5 3/10 3/5 1 7/8];
B = [ 0 0 0 0 0 1/5 0 0 0 0 3/40 9/40 0 0 0 3/10 -9/10 6/5 0 0 -11/54 5/2
-70/27 35/27 0 1631/55296 175/512 575/13824 44275/110592 253/4096];
C = [37/378 0 250/621 125/594 0 512/1771];
D = [2825/27648 0 18575/48384 13525/55296 277/14336 1/4];
xSol = zeros(2,1); ySol = zeros(2,n);
xSol(1) = x; ySol(1,:) = y;
stopper = 0; k = 1;
for p = 2:5000
K = zeros(6,n);
K(1,:) = h*feval(dEqs,x,y);
```

```
for i = 2:6
    BK = zeros(1,n);
for j = 1:i-1
    BK = BK + B(i,j)*K(j,:);
end
K(i,:) = h*feval(dEqs, x + A(i)*h, y + BK);
end
dy = zeros(1,n); E = zeros(1,n);
for i = 1:6
    dy = dy + C(i)*K(i,:);
E = E + (C(i) - D(i))*K(i,:);
end
e = sqrt(sum(E.*E)/n);
if e <= eTol
y = y + dy; x = x + h;
k = k + 1;
xSol(k) = x; ySol(k,:) = y;
if stopper == 1;
break
end
end
```

```
    if e = 0; hNext = 0.9 * h * (eTol/e)^0.2;
else; hNext = h; end
if (h > 0) == (x + hNext >= xStop )
hNext = xStop - x; stopper = 1;
end
```

```
h = hNext;
end
```

Chapter 2 (bvp4c Codes)

This MATLAB program of chapter 2 to find the solution of the stagnation-point flow of nanofluid through different utilization of thermal radiation effect using bvp4c method.

For Constant Wall Temperature (CWT)

```
function irfan-asif-cwt-nanofluid
clc
clear all
lambda=0.5;
M=0.5;
Pr=0.71;
Le=2;
Ec=0.2;
Nb=0.3;
Nt=0.5;
Rd=0;
thetaw=1.2;
sol1 = bvpinit(linspace(0, 3, 25), [1 0 0 0 0 0 0]);
sol= bvp4c(@bvpirfan, @bcirfan, sol1);
x = sol.x;
value=deval(sol,0)
```

plot(x, y(6, :),':')

val=y(7,1)

function res = bcirfan(y0, yinf)

res = [y0(1); y0(2) - 1; yinf(2) - lambda; y0(4) - 1; yinf(4); y0(6) - 1; yinf(6)];

end

function ysol= bvpirfan(x,y)

$yy1 = -y(1) * y(3) + (y(2))^2 - lambda^2 - M * (lambda - y(2));$

$coef = (1 + Rd * (1 + (thetaw - 1) * y(4))^3);$

$yy2 = (1/coef) * (-3 * Rd * (1 + (thetaw - 1) * y(4))^2 * (thetaw - 1) * y(5)^2 ....$

$+Pr * (-y(1) * y(5) - Ec * y(3)^2 - M * Ec * (lambda^2 - 2 * lambda * y(2) +$

$y(2)^2) - Nb * y(5) * y(7) - Nt * (y(5))^2));$

$yy3 = -Le * y(1) * y(7) - (Nt/Nb) * yy2;$

$ysol = [y(2); y(3); yy1; y(5); yy2; y(7); yy3];$

end

end

For Prescribed Surface Temperature (PST)

function irfan-asif-nanofluid-PST-nanofluid

clear all

close all

Pr = 7 ;

Ec = 0.2;

M = 0.5 ;

lambda = 0.5 ;

Rd = 1 ;

Nb = 0.1 ;

Le = 0 ;

Nt = 0.3 ;

function ysol = bvpex1(x,y)

yy1 =$-y(1) * y(3) + (y(2))^2 - lambda^2 - M * (lambda - y(2))$;

bcoef = $Pr/(1 + Rd)$;

yy2 = $(bcoef) * (-y(1) * y(5) + 2 * y(4) * y(2) - Nt * y(5)^2$....

$-Nb * y(5) * y(7) - Ec * y(3)^2 - M * Ec * (lambda - y(2))^2)$;

yy3 = $-Le * (y(1) * y(7) - 2 * y(2) * y(6)) - (Nt/Nb) * yy2$;

ysol = $[y(2); y(3); yy1; y(5); yy2; y(7); yy3]$;

end

function res = bcex1(y0, yinf)

res = [y0(1); y0(2) - 1; yinf(2) - lambda; y0(4) - 1; yinf(4); y0(6) - 1; yinf(6)];

end

sol1 = bvpinit(linspace(0,3,25), [1 0 0 0 0 0 0]);

sol = bvp4c(@bvpex1, @bcex1, sol1);

x = sol.x;

y = sol.y;

value = deval(sol, 0)

end

Chapter 3 (bvp4c Code)

This MATLAB program of chapter 3 to find the solution of the stagnation-point flow of nanofluid with thermal radiation effect using convective boundary condition using bvp4c method.

```
function irfan-asif-nanofluid-cwt-convective
clc
clear all
lambda=0.5;
M=0.5;
Pr=7;
Le=1;
Ec=0.2;
Nb=0.3;
Nt=0.1;
Rd=0;
thetaw=1.2;
B=0.2;
sol1 = bvpinit(linspace(0, 3 , 25), [1 0 0 0 0 0 0]);
sol= bvp4c(@bvpirfan, @bcirfan, sol1);
x = sol.x;
y= sol.y;
value=deval(sol,0)
plot(x, y(2, :),':')
vpa(-value,5)
function res = bcirfan(y0, yinf)
res = [y0(1); y0(2) - 1; yinf(2) - lambda; y0(5) + B*(1-y0(4)); yinf(4); y0(6)
- 1; yinf(6)];
```

end

function ysol= bvpirfan(x,y)

$yy1 = -y(1) * y(3) + (y(2))^2 - lambda^2 - M * (lambda - y(2));$

$coef = (1 + Rd * (1 + (thetaw - 1) * y(4))^3);$

$yy2 = (1/coef) * (-3 * Rd * (1 + (thetaw - 1) * y(4))^2 * (thetaw - 1) * y(5)^2 ....$

$+ Pr * (-y(1) * y(5) - Ec * y(3)^2 - M * Ec * (lambda^2 - 2 * lambda * y(2) +$

$y(2)^2) - Nb * y(5) * y(7) - Nt * (y(5))^2));$

$yy3 = -Le * y(1) * y(7) - (Nt/Nb) * yy2;$

ysol = [y(2); y(3); yy1; y(5); yy2; y(7); yy3];

end

end

Chapter 4 (bvp4c Codes)

This MATLAB program to find the solution of the boundary layer flow with variable fluid properties on a moving flat plate in a parallel free stream presented in chapter 4 using bvp4c method. It has two cases, case A is constant fluid properties and case B is variable viscosity. We solve both cases with bvp4c method.

Case A

function compressibleflow

epcilon = 0;

Pr = 10;

a = 1;

sol = bvpinit(linspace(0, 19, 500), [1 0 0 0 0]);

sol1 = bvp4c(@bvpirfan, @bcirfan, sol);

eta = sol1.x;

f = sol1.y ;

plot(eta, f(2, :))

value = deval(sol1, 0)

function res = bcirfan(f0, finf)

res = [f0(1) ; f0(2) - 1 + epcilon ; finf(2) - epcilon ; f0(4) - 1; finf(4)];

end

function fprime = bvpirfan(eta,f)

ff1 = $-(a/2) * (f(1) * f(3))$;

ff2 = $(-a/2) * (Pr) * (f(1) * f(5))$;

fprime = [f(2) ;f(3) ;ff1 ; f(5) ;ff2];

end

end

Case B

function compressibleflowb

epcilon = 0;

Pr = 1;

a = 1;

theetaref = -0.25 ;

sol = bvpinit(linspace(0, 19 , 25), [1 0 0 0 0]);

sol1 = bvp4c(@bvpirfan, @bcirfan, sol);

eta = sol1.x;

f = sol1.y ;

value = deval(sol1, 0)

plot(eta, f(2, :))

value = deval(sol1, 0)

function res = bcirfan(f0, finf)

res = [f0(1) ; f0(2) - 1 + epcilon ; finf(2) - epcilon ; f0(4) - 1; finf(4)];

end

function fprime = bvpirfan(eta,f)

ff1 = $-(a/2)*((theetaref - f(4))/(theetaref)) * f(1) * f(3) - (1/(theetaref - f(4))) * f(5) * f(3)$;

ff2 = $(-a/2) * (Pr) * (f(1) * f(5))$;

fprime = [f(2) ;f(3) ;ff1 ; f(5) ;ff2];

end

end